2022

# Sediment and terrestrial organic carbon budgets for the offshore Ayeyarwady Delta, Myanmar: Establishing a baseline for future change

Evan R. Flynn

S. Kuehl

Courtney K. Harris

Matthew J. Fair

Research Article

# Sediment and terrestrial organic carbon budgets for the offshore Ayeyarwady Delta, Myanmar: Establishing a baseline for future change

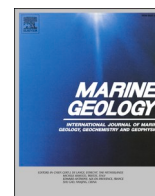Evan R. Flynn [a], Steven A. Kuehl [a,b,*], Courtney K. Harris [a], Matthew J. Fair [a]

[a] *Virginia Institute of Marine Science, Gloucester Point, VA, USA*
[b] *Xiamen University, Xiamen, China*

## ARTICLE INFO

## ABSTRACT

Large river deltas serve as globally important archives of terrestrial and shallow marine biogeochemical signatures and because of rapid sedimentation have the potential to impact global biogeochemical cycling. The Ayeyarwady Delta in Myanmar ranks as the world's third largest river delta in terms of sediment supply; however, modern increases in regional anthropogenic impacts risk severe alteration to sediment and TerrOC loads within this major system. By investigating modern sediment and terrestrial organic carbon (TerrOC) accumulation within the offshore Ayeyarwady Delta this study estimates baseline sediment and TerrOC budgets for this understudied mega-delta. Using $^{210}$Pb geochronology of 27 sediment cores collected from the continental shelf, we estimate that 405 (+52/-47) Mt of sediment, or ~70-80% of fluvial sediment discharged from the Ayeyarwady and Thanlwin rivers (the main inputs to the delta), accumulates there annually. Sediment not retained on the shelf is likely partitioned between the Ayeyarwady floodplain, shoreline accretion, and minor deep-sea export. Estimates of TerrOC (based on $\delta^{13}$C mixing models) were coupled with modern sediment accumulation rates to determine an annual burial of 1.93 (+1.09/-0.15) Mt C on the shelf, with TerrOC burial fluxes being highest in the foreset beds of the subaqueous delta, coincident with the area of highest sediment accumulation rate. Based on estimates of the Ayeyarwady and Thanlwin rivers' TerrOC delivery, an apparent ~100% of TerrOC input is preserved on the continental shelf. However, an across shelf trend of increasing TerrOC degradation with distance offshore is also observed, indicating that while the shelf has high apparent TerrOC sequestration, carbon remineralization is also occurring prior to deposition within the subaqueous delta. Based on these conflicting outcomes, we suggest that input of TerrOC from additional sources other than the Ayeyarwady and Thanlwin rivers roughly balance the observed carbon remineralization. Main additional sources of TerrOC include the Sittang and several smaller rivers, and the Ayeyarwady delta plain below the river gauging station. As anthropogenic development within the Ayeyarwady and Thanlwin watersheds continues to increase, these sediment and TerrOC budgets provide a baseline from which future changes within the offshore Ayeyarwady Delta can be monitored.

## 1. Introduction

As global sea-level rise slowed around 8 kya, the accumulation of large volumes of fluvial sediment on river-dominated ocean margins began to outpace the creation of accommodation, initiating the formation of large river deltas (Gibbs, 1981; Stanley and Warne, 1994; Meade, 1996; Saito, 2021). These deltaic deposits are repositories for terrestrial and shallow marine sediment, and serve as archives of continental-margin biogeochemical signatures due to their high preservation potential. Deltas are also implicated as a major control on global

biogeochemical cycling on both modern and geologic timescales, with ~90% of modern organic carbon burial occurring within subaqueous deltas and associated shelf deposits (Berner, 1982; Hedges, 1992; McKee et al., 2004; Burdige, 2005; Blair and Aller, 2012; Leithold et al., 2016; Bianchi et al., 2018). Rivers in Asia and Oceania transport a disproportionately large volume of sediment, and previously discharged as much as 70% of that delivered to the global ocean (Milliman and Farnsworth, 2011). This includes sediment derived from some of the world's largest river systems including the Yellow, Yangtze, Mekong, Pearl, Red, Indus, Ayeyarwady-Thanlwin, and Ganges-Brahmaputra

Rivers (Milliman and Farnsworth, 2011). These Asian mega-rivers alone account for nearly 25% of the global sediment flux to ocean margins (Milliman and Meade, 1983; Liu et al., 2009), and form many of the world's major river deltas.

In addition to their role in biogeochemical cycling, large river deltas have played a fundamental role in the development of human civilizations due to the vast agricultural, marine, and transportation resources they provide (Stanley and Warne, 1997; Day et al., 2007; Bianchi, 2016). Although human agricultural activity has been generally acknowledged to increase river sediment loads and accelerate delta growth, other human activities, including the development of river control structures, resource extraction, and floodplain engineering have caused many large deltas to subside and experience increases in severe flooding due to reduced sediment supplies and accelerated sediment compaction (Saito, 2007; Syvitski and Saito, 2007; Syvitski, 2008; Syvitski et al., 2009; Edmonds et al., 2020). Asian deltas are disproportionately affected by anthropogenic influences that result in subsidence and coastal flooding, as they tend to host megacities with dense populations such as Shanghai, Guangzhou, Bangkok, Yangon, Kolkata, and Dhaka (Syvitski and Saito, 2007; Syvitski et al., 2009). Between 2000 and 2017 the global populations living on river deltas increased by 34%, with an estimated 339 million people inhabiting river deltas by 2017 (Edmonds et al., 2020).

With populations in coastal zones only expected to continue to increase worldwide, an understanding of how large river deltas are responding to increased anthropogenic pressure is crucial (Bianchi and Allison, 2009).

Sediment budgets along a river's source-to-sink pathway have previously been used to determine how sediments are partitioned in space and over time, making them a valuable tool for understanding potential future changes from human activities (Dietrich et al., 1982; Rosati, 2005; Ramos-Scharrón and MacDonald, 2007; Warrick, 2014; Park et al., 2021). Previous studies have derived offshore sediment budgets for some of the world's largest deltas including the Ganges-Brahmaputra (Goodbred and Kuehl, 1999), the Amazon (Kuehl et al., 1986; Nittrouer et al., 1986; Nittrouer et al., 1995; Nittrouer et al., 1996), the Yangtze and Yellow (Saito and Yang, 1995; Deng et al., 2006; Qiao et al., 2017; Zhou et al., 2020), and the Mekong (Xue et al., 2010). Terrestrial organic carbon (TerrOC) budgets also elucidate the sources and sinks of organic carbon (OC) along the river-coast-marine pathway. Moreover, these budgets provide estimates of offshore OC cycling that impacts the sequestration potential of TerrOC. Such budgets have been estimated for large delta systems including the Amazon, Ganges-Brahmaputra, and East China Sea (Showers and Angle, 1986; Deng et al., 2006; Galy et al., 2007). While sediment and TerrOC budgets can be indicative of natural transport and deposition processes, they can also provide an
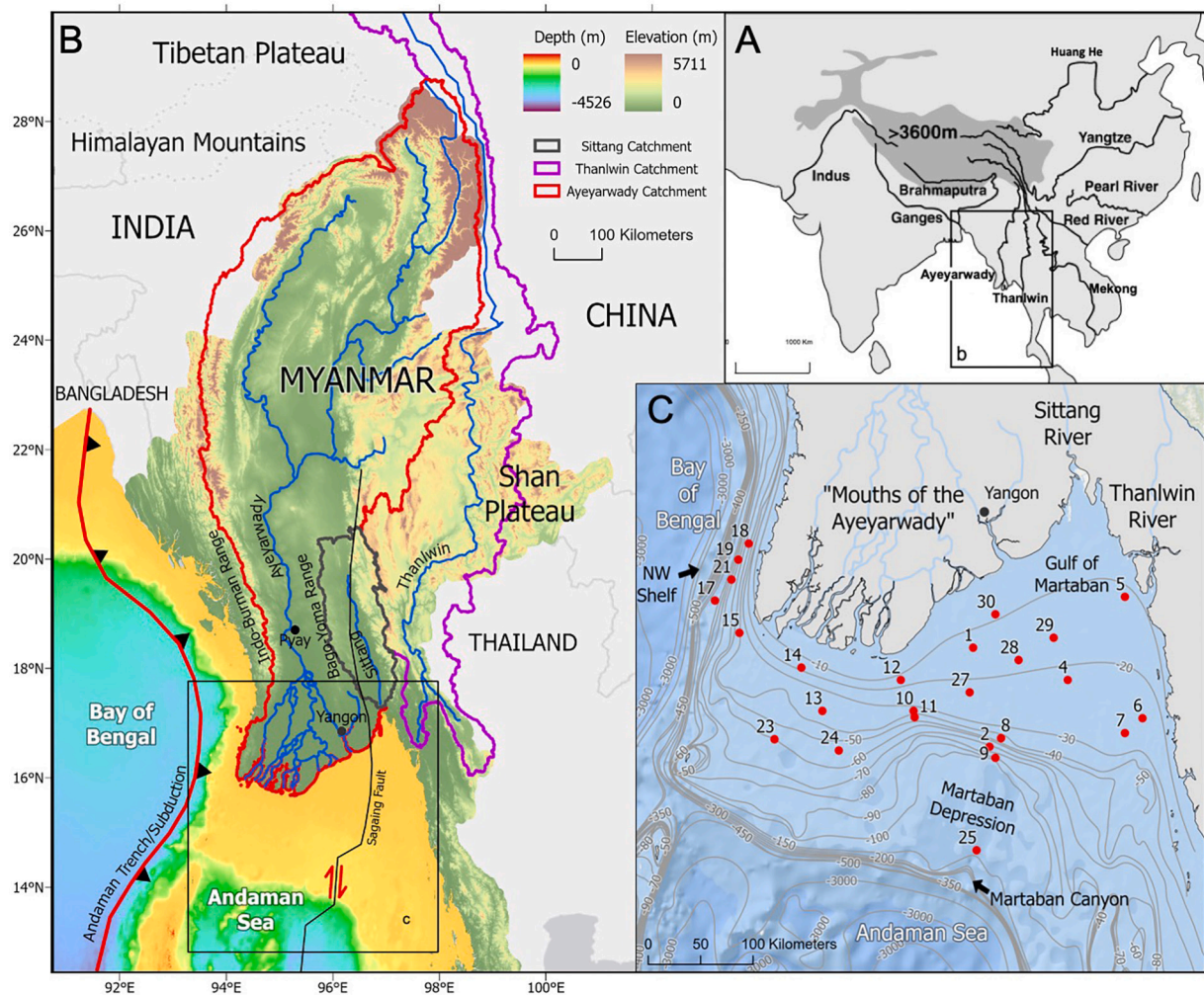


**Fig. 1.** Reference and core location maps for the Ayeyarwady Delta, Myanmar: (A) Ayeyarwady and Thanlwin Rivers along with other major rivers in Asia (Adapted from Kuehl et al., 2019); (B) Andaman Sea bathymetry and regional tectonic setting (Bathymetery from The GEBCO Digital Atlas published by the British Oceanographic Data Centre on behalf of IOC and IHO, 2003); (C) Study area with coring locations (red circles) occupied by Kuehl et al. (2019) during the 2017 research cruise. Smoothed bathymetric contours (gray lines) are shown in meters water depth (adapted from The GEBCO Digital Atlas published by the British Oceanographic Data Centre on behalf of IOC and IHO, 2003). (For interpretation of the references to colour in this figure legend, the reader is referred to the web version of this article.)

understanding of how human development may alter sources and sinks of sediment and OC, and ultimately impact the resilience of large, anthropogenically-modified delta systems.

The Ayeyarwady and Thanlwin Rivers feed the offshore Ayeyarwady Delta in Myanmar and remain the last long, free flowing rivers (i.e., undammed mainstems) in Asia outside of the Artic (Grill et al., 2019). Together they discharge onto the wide Northern Andaman continental shelf that is bisected by a major N-S striking strike-slip fault, and onto the narrow northwestern shelf that is bordered by an active subduction zone in the Bay of Bengal (Fig. 1)(Rodolfo, 1969a; Vigny et al., 2003; Curray, 2005; Sloan et al., 2017). Such tectonic activity partially drives observed submarine geomorphology and sediment accumulation patterns offshore (Kuehl et al., 2019). Although the Ayeyarwady and Thanlwin manistems are free-flowing, a recent increase in regional anthropogenic impacts, including the planned emplacement of mainstem mega-dams, have the potential to substantially alter sediment and TerrOC transport within this system (Saito, 2007; Gupta et al., 2012; Hennig, 2016). Early studies of the offshore Ayeyarwady Delta focused on surficial sediment characterization, transport, and dispersal patterns (Rodolfo, 1969b; Ramaswamy et al., 2004; Rao et al., 2005). OC fluxes from the Ayeyarwady and Thanlwin Rivers, and the surficial distribution of OC offshore have also been described (Bird et al., 2008; Ramaswamy et al., 2008; Liu et al., 2020); however, the sequestration potential of TerrOC offshore remains largely unknown, and a modern TerrOC budget has yet to be derived. Recent studies by Kuehl et al. (2019) and Liu et al. (2020) investigated sediment dispersal and accumulation on modern and Holocene timescales across the continental shelf. While Liu et al. (2020) derived a Holocene scale sediment budget and Kuehl et al. (2019) reported preliminary $^{210}$Pb accumulation rates, a modern sediment budget for the offshore Ayeyarwady Delta has yet to be estimated. This study derives sediment and TerrOC budgets in order to determine the sediment trapping and TerrOC sequestration potential offshore of the Ayeyarwady Delta. These baseline values will be crucial moving forward as future hydropower damming projects, continued mining and deforestation, and further agriculture and aquaculture development have the potential to substantially impact sediment and TerrOC transport within the Ayayarwady Delta system, resulting in changes to the ecosystem services in the region, and potentially affecting regional economics and community livelihoods (Saito, 2007; Gupta et al., 2012; Hennig, 2016; Estoque et al., 2018; Chen et al., 2020).

## 2. Regional setting

### 2.1. Regional climate and oceanography

Between mid-May and the end of September, the SW monsoon brings 90% of the region's annual rainfall and produces warm winds with speeds that reach 30 km/h and easterly surface currents (Rodolfo, 1969b). During the NE monsoon (December through February), these winds and surface currents are reversed (Ramaswamy et al., 2004; Rao et al., 2005). This reversal produces a seasonal shift throughout the Bay of Bengal and Andaman Sea from strong anticyclonic flow in surface waters during the winter to weaker cyclonic flow during the summer (Potemra et al., 1991). Wave heights also vary between the NE and SW monsoon seasons, with the highest waves (up to ~2 m) typically occurring at the peak of the SW monsoon. During inter-monsoonal periods cyclones can generate waves as high as 5 m (Besset et al., 2017). Strong semidiurnal tides with M2 (principal lunar) and S2 (principal solar) major components produce mesotidal conditions in the west along the "Mouths of the Ayeyarwady" with a tidal range of 2–4 m, and macrotidal conditions within the Gulf of Martaban in the east with a tidal range that reaches up to 7 m (Ramaswamy et al., 2004). Spring tidal currents reach up to 3 m/s within the Gulf, helping to create one of the largest perennial turbidity zones in the world. This zone spans over 45,000 km$^2$ across the Gulf of Martaban during spring tides, with the seaward turbidity front oscillating nearly 150 km in phase with spring-

neap tidal cycles (Ramaswamy et al., 2004).

### 2.2. Ayeyarwady, Thanlwin, and Sittang rivers

Substantial volumes of freshwater, sediment, and other particulate material are delivered to the Northern Andaman Sea by the Ayeyarwady, Thanlwin, and Sittang Rivers (Robinson et al., 2007; Bird et al., 2008; Furuichi et al., 2009; Baronas et al., 2020). The Ayeyarwady River is ~2170 km in length, and drains an area of 413,000 km$^3$, 95% of which is located within Myanmar (Fig. 1)(Bird et al., 2008). Rising in the Tibetan Plateau as mountainous streams draining Himalayan glaciers, the headwaters of the Ayeyarwady flow over metamorphic and plutonic bedrock (Stamp, 1940; Bender et al., 1983; Bertrand and Rangin, 2003; Garzanti et al., 2016; Giosan et al., 2018). South of the Tibetan Plateau, the Ayeyarwady flows over additional metamorphic bedrock and through volcanic hills before reaching the large, dry Central Myanmar sedimentary basin, comprised of young, non-marine sediments overlying metamorphic bedrock (Stephenson and Marshall, 1984; Mitchell, 1993; Bird et al., 2008; Chapman et al., 2015). The Ayeyarwady reaches the head of the delta plain around 290 km north of its mouths (Chapman et al., 2015). The Thanlwin River, while longer than the Ayeyarwady at ~2800 km, has a much smaller (270,000 km$^2$) and less diverse catchment (Fig. 1) (Damodararao et al., 2016). Also rising in the Tibetan Plateau, the Thanlwin flows southeast through the Yunnan Province of China, before continuing into Myanmar where it drains parts of the Shan Plateau, a topographic high rising to 1000 m and consisting primarily of Paleozoic and continental Mesozoic sedimentary rocks (Bertrand and Rangin, 2003; Chapman et al., 2015; Garzanti et al., 2016). Unlike the Ayeyarwady, the Thanlwin catchment contains deep gorges and highly resistant bedrock. This gives the Thanlwin a much smaller suspended sediment load of 159 (+78/-51) Mt/yr, compared to the 326 (+91/-70) Mt/yr transported by the Ayeyarwady (Rodolfo, 1969b; Ramaswamy and Rao, 2014; Baronas et al., 2020). Nonetheless, these rivers cumulatively transport ~485 Mt/y of sediment to the Andaman Sea (Baronas et al., 2020). The Sittang River, located between the Thanlwin and Ayeyarwady catchments, discharges into the head of Gulf of Martaban (Fig. 1), and along with other smaller rivers is estimated to deliver an additional ~50 Mt/yr of sediment to the Northern Andaman Sea; however, this estimate carries a large range of uncertainty as the Sittang and smaller rivers are not currently gauged, and estimates of sediment discharge have been derived proportionally using discharge scaling to the historical Ayeyarwady sediment load (Robinson et al., 2007; Giosan et al., 2018). Whereas these discharge estimates for the Ayeyarwady and Thanlwin are the most recently published values, earlier estimates suggest that discharge into the Gulf of Martaban and Northern Andaman Sea may be as high as >600 Mt/yr from the combined Ayeyarwady, Thanlwin, Sittang, and other smaller rivers (Robinson et al., 2007; Furuichi et al., 2009).

In addition to sediment, the Ayeyarwady and Thanlwin rivers are currently estimated to transport ~1.9(+1.4/-0.9) Mt/yr of particulate OC (POC)(Baronas et al., 2020s), a value substantially lower than the 4.6–7.7 Mt/yr POC input previously estimated by Bird et al. (2008). Baronas et al. (2020) attributes this decrease to the exclusion of coarse grains in the Bird et al. (2008) sampling methodology, and the use of higher water discharge estimates in the Bird et al. (2008) study compared to that estimated by Baronas et al. (2020). While both rivers transport POC in roughly the same amounts, they maintain characteristic OC signals due to catchment size and vegetation. The Thanlwin, which drains a catchment characterized by an alpine climate with virtually no floodplain, transports primarily C3-plant-derived POC with the average $\delta^{13}$C being −25.3‰ (Bird et al., 2008). In contrast, the Ayeyarwady, with a much larger catchment containing both alpine and savannah climates and a large floodplain, transports POC derived from both C3 and C4 plants, with C4 input being the largest during monsoon periods resulting in a weighted average $\delta^{13}$C of −24.8‰ (Bird et al., 2008). Despite potential seasonal variations in OC inputs from the

Ayeyarwady and Thanlwin catchments, the standard deviation between all samples from both rivers collected by Bird et al. (2008) during dry and wet seasons is low at ±0.36‰.

### 2.3. Ayeyarwady Delta evolution

The offshore Ayeyarwady Delta evolved over the Holocene via the deposition of Ayeyarwady, Thanlwin, and Sittang River sediments along and across the coastal zone and continental shelf (Damodararao et al., 2016; Giosan et al., 2018; Liu et al., 2020). The Ayeyarwady River has formed a large subaerial delta that covers an area of ~35,000 km$^2$ between the Indo-Burman Range and the Bago-Yoma Range (Fig. 1) (Giosan et al., 2018). Throughout the early to mid- Holocene, the subaerial accumulation of Ayeyarwady sediments formed a fluvial- and tide-dominated delta system. In the late Holocene, an increase in wave action on the emerging headland shifted the system to one of tide and wave dominance (Giosan et al., 2018; Kuehl et al., 2019). The "Mouths of the Ayeyarwady" contain four of the Ayeyarwady's five main distributary mouths and protrudes south along the western delta, whereas the eastern shoreline of the Ayeyarwady Delta is offset landward and to the north, forming a large embayment (Gulf of Martaban), likely due to an increase in tidal influences within the Gulf, as well as potential tectonic movement associated with the Sagaing fault (Fig. 1)(Giosan et al., 2018). The "Mouths of the Ayeyarwady" are also characterized by overwashed, sandy beaches which is contrast to the eastern shoreline that contains primarily fine sediments and mud flats (Giosan et al., 2018; Anthony et al., 2019).

Historical navigation charts, topographic maps, and satellite imagery suggest that the shoreline of the subaerial Ayeyarwady Delta has experienced periods of net coastal accumulation and erosion over the last 150 yrs., but that overall the coastline is more or less in a state of equilibrium with sediment deposition currently balancing subsidence and sea level rise (Hedley et al., 2009). In recent years, the western shoreline has exhibited localized erosion, primarily along the "Mouths of the Ayeyarwady" due to reductions in river sand supply associated with sand mining, channel dredging, and tributary damming, whereas the eastern shoreline has exhibited accretion, possibly from increases in fine grain sediment supply associated with large-scale coastal (mangrove) deforestation (Anthony et al., 2019). In comparison to the Ayeyarwady River, the Thanlwin River is not associated with a large subaerial delta, despite having a large sediment load. This is likely due to the extreme macrotidal conditions within the Gulf of Martaban that redistribute sediment delivered to the river's mouth offshore (Giosan et al., 2018).

The Sittang River enters the Gulf of Martaban at its apex, and is forming a bayhead delta that is actively infilling a funnel-shaped estuary (Fig. 1)(Shimozono et al., 2019). The coastlines and channels within the Sittang estuary undergo decadal to multidecadal geomorphological changes associated with lateral cyclic channel migration that is modulated by sediment discharge and the extreme flood and ebb tidal flows from the Gulf of Martaban (Shimozono et al., 2019).

### 2.4. Shelf sediment and organic carbon distribution

Distinct depositional regions are present across and along the Northern Andaman Sea and Bay of Bengal continental shelves due to spatially varying geologic, tectonic, and hydrodynamic controls, including: fluid muds in the Gulf of Martaban; a large subaqueous clinoform in the southern Gulf and Martaban Depression; a region of modern and relict sands directly off the "Mouths of the Ayeyarwady"; and a mud drape along the northwestern shelf (Rodolfo, 1969a; Rao et al., 2005; Kuehl et al., 2019; Liu et al., 2020).

The focusing of tidal currents in the Gulf of Martaban promotes extensive seabed resuspension and the formation of fluid muds in the lower half of the water column (Kuehl et al., 2019; Harris et al., 2022). Sediment cores collected from the Gulf exhibit a physically mixed layer through the top ~1 m, consist primarily of silty clays, and have low accumulation rates (Kuehl et al., 2019). The Gulf is characterized by low wt% OC that consists primarily of TerrOC (Ramaswamy et al., 2008). This may reflect substantial fluvial input, the limited success of marine primary production due to high turbidity, and the potential oxidation of sediments and OC via tidal resuspension (Ramaswamy et al., 2008; Kuehl et al., 2019).

The Martaban Depression is located seaward of the Gulf and is characterized by a distinct bathymetric low with water depths >100 m, twice as deep as adjacent shelf areas (Fig. 1)(Kuehl et al., 2019). In the depression a thick Holocene subaqueous clinoform containing predominately fine silt and clay is rapidly prograding seaward, with the highest rates of accumulation in the foreset beds (Kuehl et al., 2019). Along with tidal currents, large episodic storms have been postulated to be a major driver in the seaward sediment transport and formation of the subaqueous clinoform (Ramaswamy et al., 2004; Liu et al., 2020). There is a decrease in TerrOC and an increase in MarOC from the Gulf to the clinform, which may be due to both extensive sediment and TerrOC processing in the Gulf, and an increase in marine primary productivity offshore (Ramaswamy et al., 2008). The southern portion of the depression is dominated by relict sands, with little modern accumulation evident (Liu et al., 2020). South of the depression, the Martaban Canyon extends into the deep Andaman Basin. Previously suggested to be a conduit for sediment delivery to the deep sea (Ramaswamy et al., 2004; Rao et al., 2005), recent studies indicate that the canyon has little to no role in deep-sea sediment export, with the potential exception being sediment escaping through bottom nepheloid layers (Kuehl et al., 2019).

Off the "Mouths of the Ayeyarwady", fluvial sediment accumulates to form a mud belt in <40 m water depth, while further offshore, there is a large ~50,000 km$^2$ area of mixed modern and relict sands (Rao et al., 2005; Kuehl et al., 2019). Surficial sediments in this region contain low percentages of OC that are predominantly from marine sources (Ramaswamy et al., 2008). The low accumulation rates in this offshore region reflect exposure to large swell from the Bay of Bengal, and the focusing of wave energy around the headland at the southern extent of the Indo-Burman Range, promoting frequent sediment resuspension (Kuehl et al., 2019).

The northwestern shelf, facing the Bay of Bengal, is characterized by a ~ 20 m thick Holocene mud drape that extends across the narrow shelf at the western base of the Indo-Burman Range, thinning out with increased distance from the shoreline (Kuehl et al., 2019; Liu et al., 2020). Because of the absence of a seaward prograding clinoform in this region, sediment transport is postulated to be dispersive in the along-shelf direction (Kuehl et al., 2019). The primary sources of sediment and OC to this region are likely direct contributions from small mountainous streams that drain the Indo-Burman Range, as well as sediment transported westward from the Ayeyarwady during the NE monsoon (Ramaswamy et al., 2004; Rao et al., 2005; Damodararao et al., 2016; Kuehl et al., 2019). This region also contains the least-degraded TerrOC components compared to other offshore regions (Ramaswamy et al., 2008; Liu et al., 2020). With the mud drape extending beyond the shelf break towards the Andaman trench, it is also likely that some sediment and OC of unknown quantity is escaping into the Bay of Bengal (Kuehl et al., 2019).

### 2.5. Human impacts

While the Ayeyarwady and Thanlwin Rivers are currently relatively unimpacted by large mainstem dams, the recent effects of humans are marked (Chen et al., 2020). Mangrove deforestation is occurring at one of the fastest rates in the world in Myanmar with a 64.2% decrease in mangrove cover from 1978 to 2011 and the threat of complete mangrove depletion in the next 10 years (Webb et al., 2014; Grill et al., 2019). Terrestrial deforestation and mining are also increasing in the upper and middle reaches of the Ayeyarwady basin (Chen et al., 2020). Such human activities have been found to increase sediment supply

within the Ayeyarwady River basin (Chen et al., 2020). However, the annual extraction of ~10% of the Ayeyarwady sediment load via sediment mining and the damming of the Ayeyarwady's tributaries has led to an overall modern decrease in the Ayeyarwady-Thanlwin-Sittang sediment supply (Soe and Hammond, 2019; Chen et al., 2020). This decrease is evident as the Ayeyarwady mainstream has become less braided and tributaries have increasingly straightened since 1974 (Chen et al., 2020).

## 3. Materials and methods

### 3.1. Field data collection

In December 2017 an inter-disciplinary research cruise to the shelf region off the Ayeyarwady collected over 1500 km of high-resolution seismic data and 27 sediment cores (Fig. 1; Supplemental, Table S1) (Kuehl et al., 2019; Liu et al., 2020). As described by Kuehl et al. (2019) all cores were sub-sampled on board. Sub-samples were then dried and ground within a month of collection for laboratory analyses. Preliminary sediment accumulation rates and seismic stratigraphy were reported by Kuehl et al. (2019) and Liu et al. (2020).

### 3.2. Geochemical analyses

#### 3.2.1. $^{210}Pb$ geochronology

Methods used to determine $^{210}Pb$, $^{137}Cs$, and $^{226}Ra$ activities of sediment samples using gamma-ray spectroscopy are reported in Kuehl et al. (2019). This study re-analyzed the preliminary rates presented by Kuehl et al. (2019), by investigating small (~ 0.38 dpm/g) $^{226}Ra$ to $^{210}Pb$ calibration offsets within the dataset. Calibration offsets are defined as a deviation in supported $^{210}Pb$ activity, such that the total $^{210}Pb$ activity is higher than the supported $^{226}Ra$ activity at depths below the maximum penetration of $^{137}Cs$ and at depths where apparent excess $^{210}Pb$ activities no longer systematically decreases. Calibration offsets were determined for all applicable cores, averaged and applied to all $^{210}Pb$ core data to calculate corrected accumulation rates using constant flux, constant sedimentation rate models (Supplemental, Table S2).

#### 3.2.2. Organic carbon analysis

To allow for the calculation of OC burial from $^{210}Pb$-derived sedimentation rates, equal dry weights of all sample intervals in the region of $^{210}Pb$ activity log-linear decay for each core were composited, and dry sieved through a 500 μm sieve for stable isotope analysis. On average, five samples from each core were composited; however, compositions ranged from 2 to 16 samples depending on the penetration depth of excess $^{210}Pb$. Composited samples were prepared in duplicate by weighing ~20 mg of sample into a double-layered tin capsule and acidifying to remove carbonates. Following methods presented by Komada et al. (2008), Ramaswamy et al. (2008), and Liu et al. (2020), acidification was conducted via stepped, drop-wise addition of 1 N HCl (Supplemental, S3). Once acidified, samples were left to react in a fume hood for an additional 24 h, before being dried at 60 °C for another 24 h (Liu et al., 2020). Dried, acidified samples were pelletized to be run on a Costech Elemental Analyzer (model 4010) coupled to a ThermoFisher DeltaV Isotope Ratio Mass Spectrometer (EA-IRMS) equipped with a Conflo IV interface for continuous flow analysis of natural abundance isotopes. Isotope compositions and instrument precision and accuracy were verified against standard curves derived from a certified USGS-40 L-glutamic acid standard. Delta values were calculated relative to international standards of V-PDB and air for carbon and nitrogen, respectively. Final ratios were corrected relative to the certified USGS-40 standard. Total OC (TOC) values are reported as a percent of sediment dry weight. Reproducibility between duplicate samples was strong with the standard deviations generally being ≥0.580 for %TOC and ≥ 0.820‰ for $\delta^{13}C$, with the exception of one set of duplicates that exhibited a standard deviation of ±2.34‰ for $\delta^{13}C$; however these

duplicates did maintain a low TOC% standard deviation of ±0.007. All samples analyzed contained low concentrations of nitrogen; however, average nitrogen mass (mg) and $\delta^{15}N$ values also exhibited low standard deviations of ≥0.0113 and ≥ 0.722‰, respectively, further indicating strong reproducibility between samples (Supplemental, Table S4).

### 3.3. Grain size analysis

Grain size analysis was conducted on available samples within the depth range of excess $^{210}Pb$ log-linear decay. Grain size distribution was determined via laser diffraction using a Beckman Coulter LS 13-320. Wet samples were diluted with a 10% Calgon solution and sonicated to prevent flocculation prior to analysis. Grain size fractions were measured as percentage by volume binned into 93 intervals between <0.375 and 2000 μm. Samples were run in triplicate, with bins for each run being summed into Sand + Coarse Silt (> 16 μm), Fine Silt (3.9–16 μm), and Clay (< 3.9 μm), and the three runs being averaged for each size fraction (Supplemental, Table S8).

## 4. Results

### 4.1. Sediment accumulation rates

Of the 27 kasten cores collected and analyzed by Kuehl et al. (2019), 18 cores reached supported $^{210}Pb$ activities as identified through the lack of systematic decrease in apparent excess $^{210}Pb$ activity with depth. On average, supported $^{210}Pb$ activities below the penetration depth of $^{137}Cs$ reached 0.38 dpm/g with a standard deviation of ±0.15. Offsets were investigated in relation to grain size distribution throughout all 18 cores as well as in relation to their spatial distribution offshore. With no regional or textural trends identified, 0.38 dpm/g was subtracted from all previously reported excess $^{210}Pb$ activities before accumulation rates were derived for the present study to account for the calibration offset. Applying the offset correction decreased the preliminary accumulation rates presented by Kuehl et al. (2019) by an average of 29%; however, the spatial trends remain the same.

### 4.2. Organic carbon

Percent TOC varied offshore both along and across the Northern Andaman continental shelf, while remaining relatively consistent along the northwestern shelf in the Bay of Bengal. TOC was relatively homogenous throughout the Gulf (~ 0.6%) with a slight increase in TOC near the mouth of the Thanlwin in the eastern Gulf (Fig. 2). Moving south from the Gulf towards the Martaban Depression, %TOC increased to an offshore maximum of 1.19% before again decreasing to as low as 0.53% in the forest beds of the clinoform (Fig. 2). Off the "Mouths of the Ayeyarwady" %TOC ranged from 0.30–1.10% with the highest values occurring near the southernmost extent of the Indo-Burman Range in core KC-15 (Fig. 2). The northwestern shelf in the Bay of Bengal displayed a small range in the %TOC, from 0.82% to 1.0%, with decreasing values towards the north.

Offshore, $\delta^{13}C$ values ranged from −26.33‰ to −22.34‰ and show no obvious correlation with %TOC (Fig. 3). Within the Gulf of Martaban, $\delta^{13}C$ was typically ~ −24‰ with the exception of core KC-01 (−26.33‰; Fig. 2). In the Martaban Depression $\delta^{13}C$ became more enriched, reaching −22.88‰ in the most seaward core collected from the base of the subaqueous clinoform (KC-09; Fig. 2). The most enriched $\delta^{13}C$ value was found offshore of the "Mouths of the Ayeyarwady" (KC-24: −22.34‰; Fig. 2). Closer to the shoreline, $\delta^{13}C$ became more depleted reaching −25.46‰ in core KC-14 directly off the central portion of the Ayeyarwady distributaries (Fig. 2). Similar to TOC, the northwestern shelf again showed relatively little variation of $\delta^{13}C$, ranging from −24.36‰ to −23.22‰ (Fig. 2). Molar N/C ratios and $\delta^{15}N$ ranged from 0.09–0.1 and 0.906–3.73‰ respectively and show no spatial distribution trend either along or across shelf. Additionally, N/C
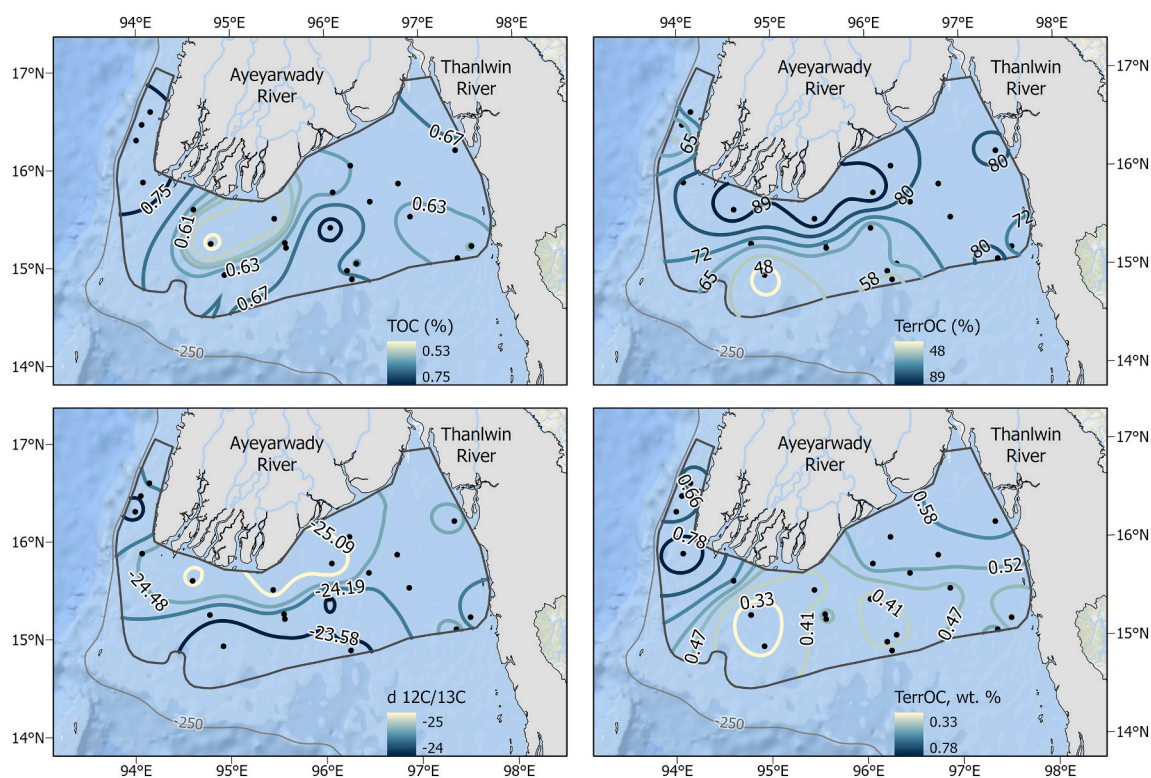
**Fig. 2.** Spatial distribution of %TOC, terrestrial fraction of TOC, δ13C, and TerrOC by wt% within the region of modern offshore sediment accumulation. Coring locations are indicated by black circles. The shelf break is indicated by the gray bathymetry contour at 250 m depth.
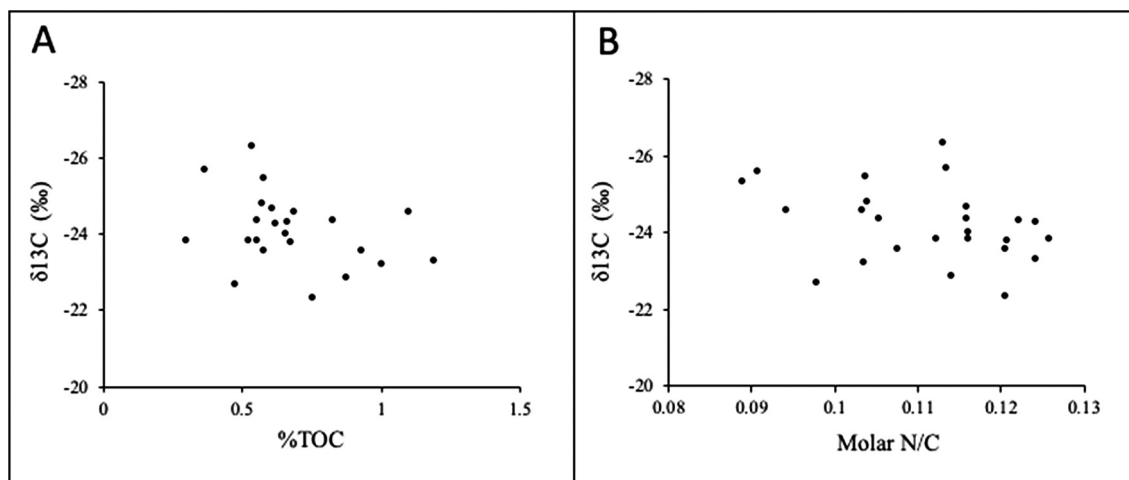


**Fig. 3.** Scatter plots relating δ13C to (A) %TOC and (B) N/C for all samples.

only minimally correlates with δ13C for the samples analyzed (Fig. 3). This may be explained by low nitrogen wt% (∼ 0.088%) in all samples analyzed, thus preventing the use of N/C or δ15N as a reliable source indicators.

### 4.3. Grain size

The average mud content of sediment cores was the highest within the Gulf of Martaban and the Martaban Depression, reaching up to 86% in the southeastern Gulf (Fig. 4). Towards the east, off the "Mouths of the Ayeyarwady" mud content reached a low of 61% before again increasing to over 70% along the northwestern shelf. The spatial distribution of % TOC did not strongly correlate with core-averaged mud content across

the entire study area, as mud content was highest in the Gulf while % TOC was highest along the northwestern shelf (Figs. 2 & 4). While this was unexpected, we suggest it may be due to the limited availability of samples suitable for grain size analysis. Because not all samples used to produce composites for OC analysis were available for grain size analysis, core-averaged grain size is not fully representative of the composited OC sample, which likely impacts any correlation between grain size and %TOC.
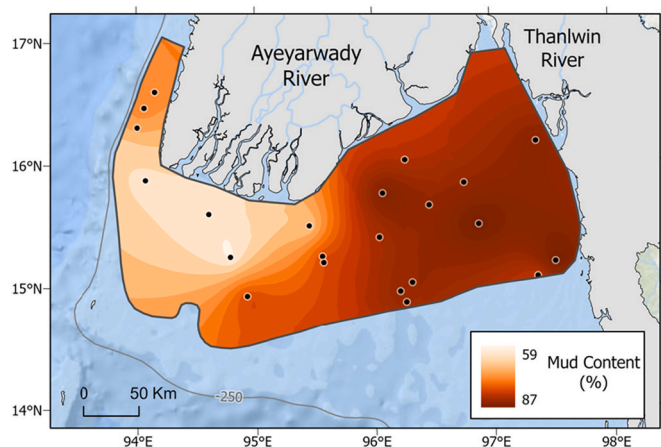
**Fig. 4.** Spatial distribution of mud content. Coring locations are indicated by black circles. The shelf break is indicated by the gray bathymetry contour at 250 m depth.

## 5. Discussion

### 5.1. Modern sediment budget

[210]Pb accumulation rates were analyzed to estimate the modern (~ 100 yr) accumulation of sediment on the continental shelf of the offshore Ayeyarwady delta. Observed average accumulation rates were plotted in ArcGIS Pro and interpolated using Empirical Bayesian Kriging (EBK) methods (Supplemental, S5). The analysis was performed over the area of deposition (area in Fig. 5), which was assumed to extend from the shoreline to the offshore boundary of the deposit as defined below. The observations provided 27 data points distributed within the Gulf of Martaban, Martaban Depression, "Mouths of the Ayeyarwady", and northwestern shelf. As described below, the observed values were supplemented with modeled accumulation rates in areas of low data density; and with assumed low accumulation rates along the offshore boundary of the deposit. The EBK interpolation of average observed and modeled rates produced 32 contour intervals. To determine the mass of sediment accumulating within each interval, the geodesic area between

each contour was multiplied by the average accumulation rate of bounding contour intervals and a sediment bulk density of 0.795 g/cm^{3}, which was calculated from the average grain size and porosity of sediments offshore as bulk density measurements were not available for the cores analyzed in this study (Supplemental, S6; Jia et al., 2018). Mass accumulation rates from all intervals were then summed to produce the shelf-wide budget, giving an average mass accumulation of 405 Mt/yr on the continental shelf.

The boundary of accumulation on the shelf, shown in Fig. 5 was chosen as follows. Along the northwestern shelf, the limit of modern accumulation was determined by regional bathymetry (i.e., shelf break, ~ 250 m) as seismic profiles indicate that accumulation extends beyond the shelf at least to the upper slope (Kuehl et al., 2019; Liu et al., 2020). South of the Gulf of Martaban, the limit of accumulation was established using seismic profiles which show a sharp, well-defined boundary between the mud-clinoform and offshore relict sands (Liu et al., 2020). However, off the "Mouths of the Ayeyarwady", the seismic boundary is less definitive (Liu et al., 2020), thus the offshore limit of modern sediment accumulation was specified based on consideration of sediment transport dynamics. A hydrodynamic model of the study site indicated that time-averaged bed shear stresses decreased with offshore distance off the "Mouths of the Ayeyarwady" (Fair, 2021). As sediment is dispersed seaward from the river inputs and shear stresses drop, eventually the critical threshold is reached and further seaward transport ceases. The lowest accumulation rates occur where bed stress across-shelf approached ~0.1 Pa (Fig. 5). Therefore, the offshore boundary of accumulation was chosen as the depth at which time-averaged modeled bed shear stress fell below 0.1 Pa.

For the interpolation, modeled accumulation rate points were included in areas of low observed data-density that exhibited high prediction error, as well as along the accumulation boundary to improve interpolation predictions as follows. Modeled points along the seaward accumulation boundary were set to 0 cm/yr to define the limit of accumulation. Given the similarity between observed rates within the Gulf of Martaban, along the northwestern shelf, and off the "Mouths of the Ayeyarwady", modeled points in these regions were assigned rate values based on the nearest surrounding observed accumulation rates. In contrast, modeled points south of the Gulf of Martaban and in the Martaban Depression clinoform were assigned rate values based on seismic profile interpretation of clinoform beds as observed rates varied
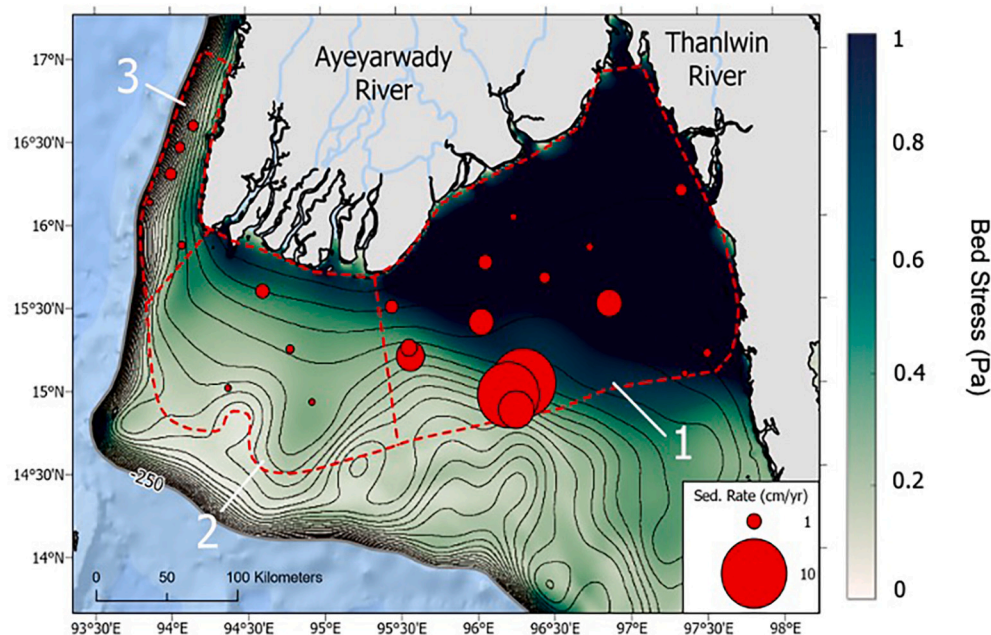


**Fig. 5.** Modeled time-averaged bed stress from combined wave and tidal forcing for August 2017 shown in relation to ^{210}Pb-derived sediment accumulation rates. Regions of accumulation are delineated by the red-dashed lines. The shelf break is identified at 250 m depth using the smoothed model-derived bathymetry. Other smoothed bathymetric contours are represented as black lines across the shelf. Limits of accumulation by region are as follows, 1) defined by seismic profiles (Liu et al., 2020), 2) by the relationship between bed stress and accumulation, and 3) by the modeled 250 m bathymetric contour. Model results from Fair, 2021. (For interpretation of the references to colour in this figure legend, the reader is referred to the web version of this article.)

in accordance with the expected progressive decrease from clinoform foreset to bottomset beds based on seismic profiles. Including modeled rates improved all interpolations resulting in Root Mean Square Error (RMSE) ≤ 0.43 and cross validation means ≤0.082, indicating that on average predicted rates are within ~0.5 cm/yr of the observed and there is no tendency towards the over or under prediction of rates.

In summary, the analysis concluded that the sediment accumulation rate averaged 405 Mt/yr over a 100-yr timescale. To estimate potential error in the budget, EBK interpolations were also produced for observed minimum and maximum accumulation rates that were derived using the standard error of the linear regression of excess $^{210}$Pb activities, resulting in a final estimate of 405 (+52/-47) Mt of sediment accumulating on the shelf annually (Table 1; Fig. 6). This estimate likely contains the maximum error in total sediment accumulation due to the use of systematic minimum and maximum $^{210}$Pb accumulation rates.

Previous studies in the region have suggested that fluvial sediment is transported by surface currents from the "Mouths of the Ayeyarwady" to the northwestern shelf in the Bay of Bengal during the NE monsoon (Rodolfo, 1969a; Ramaswamy et al., 2004; Rao et al., 2005; Kuehl et al., 2019; Liu et al., 2020). However, elemental analyses of sediments from the northwestern shelf have indicated that this region may also be receiving fluvial sediment from sources other than the Ayeyarwady and Thanlwin Rivers, such as small, mountainous streams draining the Indo-Burman Range (Damodararao et al., 2016). Therefore, an alternate Ayeyarwady-Thanlwin sediment budget excluding the northwestern shelf was also derived. This alternative budget utilizes the offshore trace of the Indo-Burman Range as the dividing boundary, extending south from the subaerial range along the western "Mouths of the Ayeyarwady" to the Andaman and Nicobar Islands, thereby essentially restricting the budget to the Northern Andaman Sea shelf (Fig. 6). Accumulation within this area is found to be 391 ± 48 Mt/yr, indicating that only ~14 Mt/yr, or ~ 3% of the total sediment budget, accumulates on the northwestern shelf, making it a minor sink for Ayeyarwady and Thanlwin derived sediment in any case (Table 1).

To determine the shelf trapping efficiency for the offshore Ayeyrwady Delta we compared the river sediment discharge estimate of ~485 Mt/yr for the Ayeyarwady and Thanlwin by Baronas et al. (2020) to the shelf-wide accumulation rate derived here. We opted to use the Baronas et al. (2020) discharge rate (as opposed to earlier estimates) as it not only utilizes the most recent measurements of the Ayeyarwady and Thanlwin sediment loads, but also derives the first sediment rating curve for the Thanlwin. Based on this comparison, we calculate an average shelf trapping efficiency of ~80%. This estimate is largely unimpacted by the exclusion of the northwestern shelf, because of the small overall fraction accumulating there. However, our estimate of trapping efficiency is likely an upper limit, as additional input from smaller, ungauged rivers, such as the Sittang River, were not included. If we take into account the additional estimated 50 Mt/yr of sediment from the Sittang and other small rivers (Robinson et al., 2007), average trapping efficiency is only decreased to ~70%. Therefore, based on average estimates of sediment input and retention, the shelf off the Ayeyarwady

appears to be a major repository for the rivers' sediment delivery. Fluvial sediment that is not retained on the shelf may escape to the deep sea via the northwestern shelf, or may contribute to floodplain or localized shoreline accretion along the subaerial Ayeyarwady Delta (Fig. 7). For example, Glover et al., 2021 estimated that 20–60% of the Ayeyarwady mainstem sediment load is retained in the floodplain during high flow, indicating that it may provide a substantial sink for Ayeyarwady sediments that are not transported offshore.

A recent study by Liu et al. (2020) used seismic interpretation to estimate that $1.29 \times 10^6$ Mt of sediment has accumulated on the shelf off the Ayeyarwady and Thanlwin Rivers over the last 6 kyr, equating to an average of 215 Mt/yr. Compared to our modern sediment budget (~ 405 Mt/yr) this would seem to suggest that offshore sediment accumulation has increased over the late Holocene. While we can't rule out changes in river discharge or offshore erosion over time, the difference between the Holocene and modern budgets can in large part be attributed to the evolution of the Ayeyarwady Delta plain. Over the last 6kyr the delta plain has prograded ~80 km seaward to the present shoreline (Giosan et al., 2018). Because Liu et al.'s (2020) Holocene budget is restricted to the present-day offshore area, it does not account for accumulation within paleo-offshore deposits that form the base of the mid-late Holocene delta plain. Thus, the lack of accounting for the paleo-offshore deposits in the Holocene budget probably explains the large discrepancy with our modern budget.

## 5.2. Modern terrestrial organic carbon budget

Modern TerrOC sequestration on the shelf was calculated using accumulation rates derived from $^{210}$Pb geochronology along with estimates of %TerrOC produced from a simple two-end-member $\delta^{13}$C mixing model as shown in Eq (1):

*($\delta^{13}$C Marine end-member) – ($\delta^{13}$C Observed) / ($\delta^{13}$C Marine end-member) - ($\delta^{13}$C Terrestrial end-member) = Estimated % TerrOC* (1)

The marine end-member is the average $\delta^{13}$C from core tops collected within the Andaman Sea Basin and Bay of Bengal (−20.5‰), and is representative of typical $\delta^{13}$C for marine phytoplankton (Fontugne and Duplessy, 1986). For the terrestrial end-member we opted to use the average $\delta^{13}$C of POC for the Ayeyarwady and Thanlwin presented by Bird et al. (2008)(−25.1‰). Because mixing models can be sensitive to end-member selection, $\delta^{13}$C values ±1 standard deviation from average marine and terrestrial end-members were used to identify a likely range of %TerrOC for each core, resulting in an average difference between minimum and maximum %TerrOC of ~19% (Fontugne and Duplessy, 1986; Bird et al., 2008).

Although most of the stations had $\delta^{13}$C values within the range of chosen end-members, three exhibited more depleted $\delta^{13}$C than the terrestrial end-member (these were considered to be 100% TerrOC) (Fig. 2). This may be explained by the preservation of low discharge signatures in the sediment record as periods of low discharge within the Ayeyarwady are associated with increased input of forest/alpine-derived POC, which is depleted relative to the savannah-derived POC that is more abundant during periods of high discharge (Bird et al., 2008). Unfortunately, the low correlation between N/C and $\delta^{13}$C (Fig. 3) prevented us from successfully utilizing N/C ratio mixing models to verify our $\delta^{13}$C-based %TerrOC estimates. Ramaswamy et al. (2008) found a similar relationship between N/C and $\delta^{13}$C in surficial sediments offshore. This is potentially due to marine biologically-driven nitrogen cycling that may alter terrestrial nitrogen signals in fluvial sediment prior to deposition offshore. Additionally, due to the low nitrogen content detected in all samples, $\delta^{13}$C is likely the most reliable indicator of TerrOC signals for this study.

To derive TerrOC burial fluxes, the estimated %TerrOC was multiplied by the respective %TOC, sediment bulk density (0.795 g/cm$^3$), and sediment accumulation rate (Supplemental S4). Derived burial fluxes were then interpolated using EBK methods to best estimate TerrOC sequestration within the boundary of modern sediment accumulation.
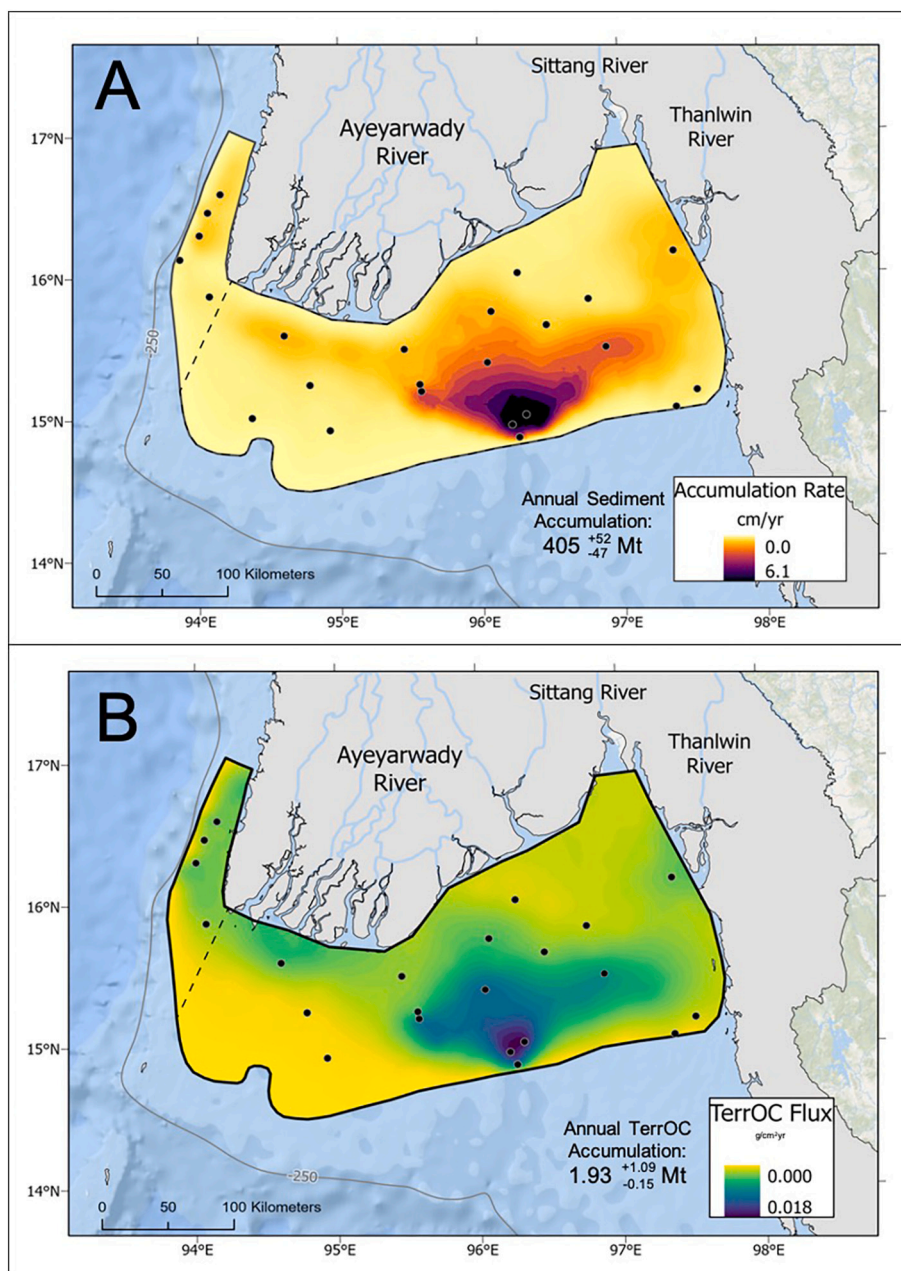
**Table 1**
Summary values for modern sediment and TerrOC budgets for the offshore Ayeyarwady Delta. The range of uncertainty for mass accumulations derived from minimum and maximum sediment and TerrOC fluxes is given in parentheses.

| | Average annual offshore accumulation (Mt/yr) | |
| --- | --- | --- |
| | Including NW shelf | Excluding NW shelf |
| Holocene sediment budget (Liu et al., 2020) | 215 | 200 |
| Modern sediment budget (this study) | 405 (+52/-47) | 391 ± 48 |
| Modern TerrOC budget (this study) | 1.93 (+1.09/-0.15) | 1.81 (+1.09/-0.10) |

**Fig. 6.** ArcGIS Pro EBK interpolations showing: (A) ^{210}Pb-derived sediment accumulation rates and integrated sediment budget; (B) TerrOC burial fluxes and integrated TerrOC budget. Coring locations are shown as black circles. The shelf break is indicated by the gray bathymetry contour at 250 m depth. The alternative budget boundary between the Northern Andaman shelf and the northwestern shelf is shown as the dashed line (see Discussion).

Modeled points were again included to improve interpolation predictions for locations of low data density as described for accumulation rates in section 5.1. To account for error in the TerrOC burial fluxes, interpolations of minimum and maximum fluxes were also produced from the respective range of %TerrOC and sediment accumulation rate for each core. All EBK interpolations demonstrate RMSE $\leq 0.0019$, and cross validation means $\leq 0.00023$, indicating that predicted burial fluxes within each interpolation align with the observed TerrOC burial fluxes (Supplemental S5). Using the same methods as the sediment budget, it is estimated that 1.93 (+1.09/-0.15) Mt/yr of TerrOC is accumulating on the continental shelf (Table 1), with the highest TerrOC burial fluxes found within the foreset beds of the subaqueous clinoform (where sediment accumulation rates are also highest)(Fig. 6). TerrOC budgets were also constructed with the exclusion of the northwestern shelf, resulting in a decrease to 1.81 (+1.09/0.10)Mt/yr of TerrOC

accumulating offshore (Table 1). These estimates also likely represent the maximum error in TerrOC accumulation on the shelf due to the use of minimum and maximum accumulation rates and the variations in end-members used to derive %TerrOC for each core location.

Comparing our estimated rate of offshore TerrOC accumulation to the Baronas et al. (2020) POC input estimate apparently suggests that on average ~ 100% of TerrOC input is being sequestered offshore. Exclusion of the northwestern shelf does not substantially alter this budget, decreasing TerrOC sequestration to ~95%. Again, these estimates should be viewed as an upper limit of sequestration potential, as input of POC from ungauged sources such as the Sittang River is not included in Baronas et al.'s (2020) estimate of POC discharge. Furthermore, because the Baronas et al. (2020) estimates were made at Pyay (Fig. 1), they ignore any potential TerrOC input from the entire lower delta plain of the Ayeyarwady. Event-driven deposition (i.e., deposition via
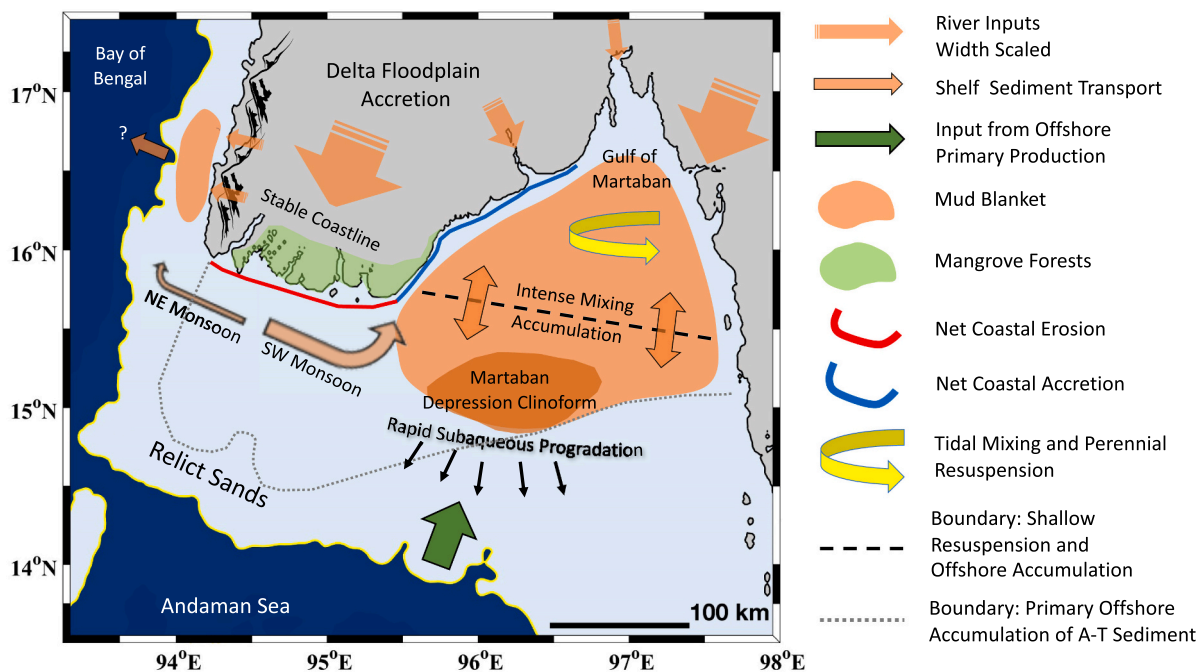
**Fig. 7.** Conceptual diagram of sediment and TerrOC input, transport, and deposition offshore of the Ayeyarwady Delta (Adapted from Kuehl et al., 2019). Zones of net coastal sediment erosion and accretion are based on Anthony et al. (2019) and Chen et al. (2020).

monsoons) may also facilitate the high apparent TerrOC sequestration within the clinoform as large volumes of POC and sediment are rapidly discharged and deposited offshore, potentially allowing large quantities of TerrOC to bypass the tidally mixed Gulf where degradation is likely to occur (Fig. 7).

Despite the high apparent sequestration of OC on the shelf, our $\delta^{13}$C-derived TerrOC values suggest that some carbon remineralization is occurring. This is evidenced by a 20% decrease between the wt% of TerrOC in the relatively homogenous Gulf and that of the Martaban Depression, providing evidence for the partial remineralization of TerrOC with increasing distance offshore (Fig. 2). While tidal mixing within the Gulf likely acts to remove TerrOC via resuspension and oxidation prior to deposition within the clinoform, the "priming effect" may also increase oxidation of TerrOC at the southern edge of the Gulf as increased light availability in this region allows for the production of labile marine OC which when mixed with recalcitrant TerrOC may accelerate remineralization (Fig. 7) (Griffith et al., 2010; Bianchi, 2011; Ramaswamy and Rao, 2014). We thus suggest that our estimated ~100% TerrOC sequestration is attributed to additional POC input from ungauged rivers and from the Ayeyarwady floodplain, driving up TerrOC burial fluxes offshore, while the partial oxidation of TerrOC through tidal mixing and "priming" acts to modulate the accumulation of TerrOC from the Ayeyarwady, Thanlwin, and any additional sources.

Interestingly, the northwestern shelf exhibits the highest wt%TerrOC (0.75%) found in the study area, suggesting high TerrOC preservation potential; however, the budgets derived here indicate that this region does not accumulate substantial amounts of sediment from the Ayeyarwady-Thanlwin Rivers. We therefore suspect this region is likely a major sink for relatively undegraded TerrOC from the Indo-Burman Range, while being only a minor sink for Ayeyarwady and Thanlwin derived POC (Fig. 7). The northwestern shelf also exhibits the highest % TOC of all offshore regions and enriched $\delta^{13}$C relative to the terrestrial end-members (Fig. 2). This may be explained by an increase in marine primary production along the northwestern shelf enriching $\delta^{13}$C and increasing the overall %TOC, thereby diluting terrestrial signatures. An important caveat here is the possibility that the terrestrial Ayeyarwady-

Thanlwin $\delta^{13}$C end-members used in this study do not reflect terrestrial sources from the Indo-Burman Range, which could affect the mixing model results for the northwestern shelf and hence the estimated TerrOC values. However, given the small fraction of sediment sequestered in the northwestern shelf, any discrepancy would have minimal effect on the above budget calculations.

### 5.3. Global implications

The modern Ayeyarwady-Thanlwin sediment budget presented here estimates that 405 (+52/-47) Mt, or ~ 70–80% of the fluvial sediment load, is trapped on the continental shelf annually, with the remaining sediment being partitioned between floodplain accumulation, localized shoreline accretion, and possible export to the Bay of Bengal. Given estimates by Glover et al. (2021), we anticipate that majority of the remaining Ayeyarwady sediment load (~1/3) is trapped within the Ayeyarwady floodplain, which is similar to sediment partitioning for other large delta systems in tectonically active regions, such as the Ganges-Brahmaputra (Fig. 8) (Goodbred and Kuehl, 1999). Because the Thanlwin River has virtually no floodplain to allow for the accumulation or processing of sediments (Bird et al., 2008), the majority, if not all, of its sediment load is delivered to the Gulf of Martaban.

Our estimate of ~70–80% shelf trapping efficiency for Ayeyarwady and Thanlwin River sediment is also comparable to that of the Amazon River Delta which reaches ~70% including its proximal clinoform and distal mobile mud belt depocenters (Fig. 8) (Kuehl et al., 1986; Nittrouer et al., 1986; Nittrouer et al., 2021). In the case of the Amazon, high volumes of water discharge, tidal forcing, and estuarine-like circulation on the continental shelf drive the formation of fluid muds that extend from the mouth of the Amazon to the subaqueous clinoform on the continental shelf during periods of rising and high discharge (Kineke and Sternberg, 1995). These fluid muds trap sediment on the shelf and are associated with relatively low sediment accumulation rates, but can provide substantial sources of sediment to the clinoform through the episodic release of muds via sediment gravity flows (Kuehl et al., 1986; Kuehl et al., 1995; Dukat and Kuehl, 1995; Allison et al., 2000). It is
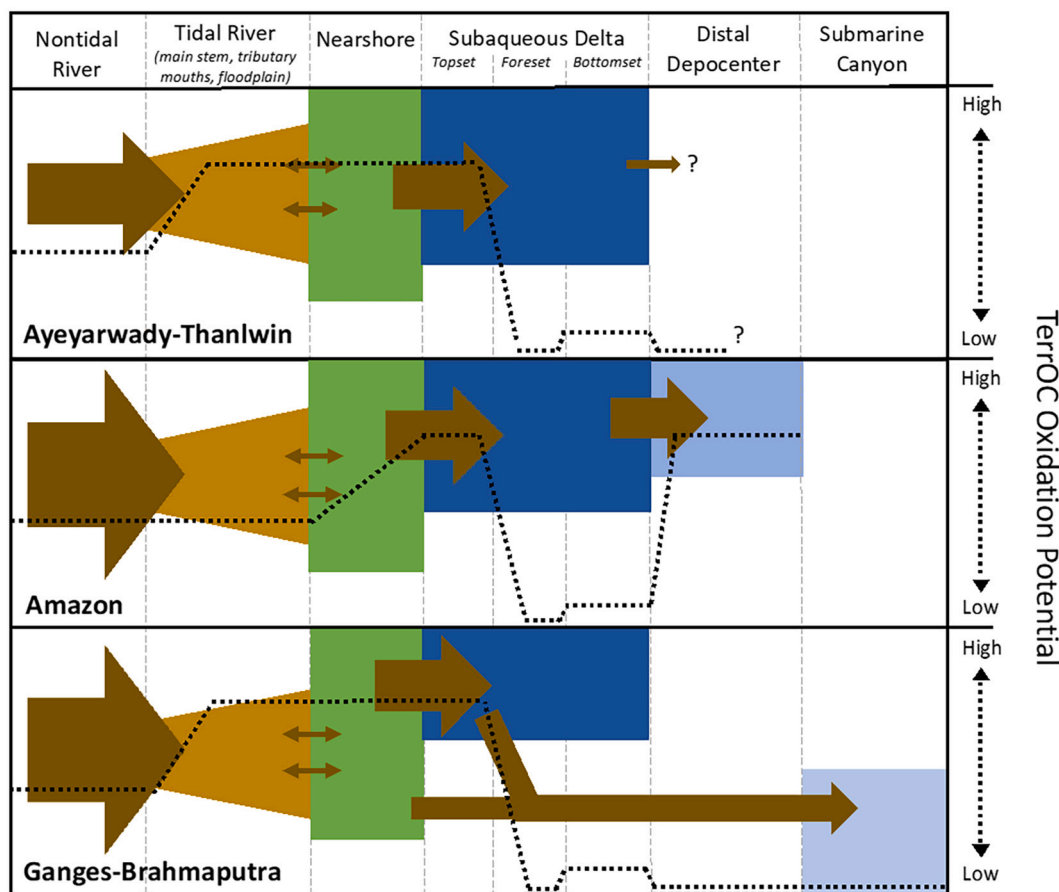
**Fig. 8.** Conceptual diagram comparing sediment and TerrOC accumulation offshore of the Ayeyarwady-Thanlwin, Ganges-Brahmaputra, and Amazon River Deltas. Brown arrows are scaled relatively to the mass of sediment entering each section of the river-coast-marine pathway from fluvial source to offshore sinks. Boxes are also scaled relatively to the mass of sediment accumulating in each region. Relative (low to high) TerrOC oxidation potential within each section is shown by the dotted black line. Question marks are included within the Ayeyarwady-Thanlwin system to include the potential for minor export of sediment and TerrOC to the deep sea on the northwestern shelf. (For interpretation of the references to colour in this figure legend, the reader is referred to the web version of this article.)

anticipated that mechanisms similar to those in the Amazon may be driving fluid mud formation and clinoform progradation in the Gulf of Martaban and Martaban Depression, given the extreme tides and intense seabed mixing. Sediment trapping and intense mixing within fluid muds can also result in the efficient oxidation of OC (Blair and Aller, 2012; Bianchi et al., 2018). Nearly 1/3 of TerrOC within fluid muds offshore of the Amazon has been found to remineralize prior to deposition within the Amazon subaqueous delta (Aller et al., 1996; Aller, 1998; Showers and Angle, 1986). This may be comparable to the Ayeyarwady considering the evidence of extensive mixing and fluid muds present within the Gulf of Martaban (Kuehl et al., 2020; Harris et al., 2022), and the potential for linkage between the Gulf and the clinoform, as is found within the Amazon (Fig. 8). However, the scale and spatial distribution of fluid muds is vastly different between these two systems as fluid mud formation offshore of the Ayeyarwady seems to occur within a partially enclosed Gulf that is bounded seaward by a proximal depocenter (i.e., the Martaban Depression clinoform) (Fig. 6), whereas the Amazon exhibits a mobile mud belt that extends not only seaward to a proximal depocenter, but also north ~1600 km to a distal depocenter that faces continuous exposure to open ocean processes (Fig. 8) (Nittrouer et al., 2021). Therefore, the extended transport and processing within the fluid mud belt in the Amazon may allow for more extensive TerrOC remineralization than offshore of the Ayeyarwady (Figs. 7, 8). This is supported by comparing the 20% decrease in wt%TerrOC between the Gulf of Martaban and the clinoform identified in this study, to the ~1/3 TerrOC remineralization identified in the Amazon.

At present high-stand sea level conditions, the Ayeyarwady and

Amazon Delta systems are both disconnected from the submarine canyons that were incised by the rivers under previous low-stand conditions (Kuehl et al., 2019; Nittrouer et al., 2021). Conversely, the Ganges-Bramaputra Delta exports roughly 1/3 of its sediment load to the deep sea via a submarine canyon (i.e. the Swatch of No Ground) (Fig. 8) (Goodbred and Kuehl, 1999). This connectivity has significant implications not only for the accumulation of fluvial sediment, but also TerrOC. While deep sea export through the Swatch of No Ground limits regional sediment shelf trapping, it allows for the efficient sequestration of substantial amounts of undegraded TerrOC as indicated by the roughly equal loading of TerrOC on sediments in the Bengal fan as compared with Ganges-Brahmaputra River sediments (Galy et al., 2007). In contrast, the Martaban Canyon is not presently a conduit for sediment export to the deep sea, helping to explain the higher regional shelf trapping of ~70–80%, as compared to ~1/3 for the Ganges-Brahmaputra system (Fig. 8) (Goodbred and Kuehl, 1999; Kuehl et al., 2019; Liu et al., 2020). For the Ayeyarwady system, the most likely escape path of sediment to the deep sea occurs along the northwestern shelf, however, given the results of our budget analysis, this escape of Ayeyarwady-Thanlwin sediment is likely minimal (Fig. 8).

Annual sediment fluxes of other large Asian rivers such as the Yellow, Yangtze, Indus, Red, and Mekong have decreased by 20–90%, largely due to increased damming over the late 20th century (Yang et al., 2011; Gupta et al., 2012; Binh et al., 2020; Ve et al., 2021). Not only does dam construction decrease sediment loads within these systems, but also creates anthropogenic reservoirs that sequester a substantial amount of POC as is shown through the sequestration of 4.9 Mt of biospheric POC

by dams along the Yangtze in the last 50 years alone (Dean and Gorham, 1998; Battin et al., 2009; Liu et al., 2014). Additionally, the modern expansion of aquaculture and rice agriculture has driven an increase in mangrove deforestation in many of Asia's tropical and subtropical deltas, further increasing delta vulnerability through coastal erosion (Richards and Friess, 2015). While the Ayeyarwady and Thanlwin have not undergone extensive damming on the river mainstems, other anthropogenic impacts such as deforestation (mangrove and terrestrial) and terrestrial mining have increased fluvial sediment loads and decreased mangrove carbon stocks in recent decades (Estoque et al., 2018; Chen et al., 2020). Despite 25% of delta growth globally being attributed to terrestrial deforestation-induced sediment supply increases, river damming has still reduced sediment fluxes by more than 50% for nearly 1000 deltas worldwide (Nienhuis et al., 2020). Thus, the impending development of hydropower dams along the Ayeyarwady-Thanlwin River mainstems, the continued removal of mangrove forests, and sediment mining, may drastically alter the sediment and TerrOC loads of these rivers, impacting offshore accumulation of both sediment and TerrOC (Chen et al., 2020). This also has the potential to result in decreased coastline stability at the "Mouths of the Ayeyarwady", decreased coastal carbon stocks, shifts in the location of main distributaries on the delta plain, and even the erosion of the subaqueous clinoform, all of which could greatly impact local communities residing along the coast of Myanmar and on the delta plain. Over 54 million people currently depend on the resources provided by the Ayeyarwady and Thanlwin Rivers, and ~ 30% of them live on the Ayeyarwady Delta plain (World Population Review, 2019). This population is vulnerable to severe coastal inundation as the catchments and river mouths of the Ayeyarwady and Thanlwin Rivers continue to be anthropogenically modified (Syvitski and Saito, 2007; Syvitski et al., 2009).

## Data Availability

Datasets related to this article can be made available upon request.

## Declaration of Competing Interest

The authors declare that they have no known competing financial interests or personal relationships that could have appeared to influence the work reported in this paper.

## Acknowledgements

## Appendix A. Supplementary data

Supplementary data to this article can be found online at https://doi.org/10.1016/j.margeo.2022.106782.

## References

Aller, R.C., 1998. Mobile deltaic and continental shelf muds as suboxic, fluidized bed reactors. Mar. Chem. 61, 143–155. https://doi.org/10.1016/S0304-4203(98)00024-3.

Aller, R.C., Blair, N.E., Xia, Q., Rude, P.D., 1996. Remineralization rates, recycling, and storage of carbon in Amazon shelf sediments. Cont. Shelf Res. 16, 753–786. https://doi.org/10.1016/0278-4343(95)00046-1.

Allison, M.A., Lee, M.T., Ogston, A.S., Aller, R.C., 2000. Origin of Amazon mudbanks along the northeastern coast of South America. Mar. Geol. 163, 241–256. https://doi.org/10.1016/S0025-3227(99)00120-6.

Anthony, E.J., Besset, M., Dussouillez, P., Goichot, M., Loisel, H., 2019. Overview of the Monsoon-influenced Ayeyarwady River delta, and delta shoreline mobility in response to changing fluvial sediment supply. Mar. Geol. 417, 106038 https://doi.org/10.1016/j.margeo.2019.106038.

Baronas, J.J., Stevenson, E.I., Hackney, C.R., Darby, S.E., Bickle, M.J., Hilton, R.G., Larkin, C.S., Parsons, D.R., Myo Khaing, A., Tipper, E.T., 2020. Integrating suspended sediment flux in large alluvial river channels: application of a synoptic rouse-based model to the Irrawaddy and Salween Rivers. J. Geophys. Res. Earth Surf. 125 https://doi.org/10.1029/2020JF005554.

Battin, T.J., Luyssaert, S., Kaplan, L.A., Aufdenkampe, A.K., Richter, A., Tranvik, L.J., 2009. The boundless carbon cycle. Nat. Geosci. 2, 598–600. https://doi.org/10.1038/ngeo618.

Bender, F., Bannert, D., Bannert, D.N., 1983. Geology of Burma. In: Gebr. Borntraeger.

Berner, R.A., 1982. Burial of organic carbon and pyrite sulfur in the modern ocean: its geochemical and environmental significance. Am. J. Sci. (United States) 282. https://doi.org/10.2475/ajs.282.4.451.

Bertrand, G., Rangin, C., 2003. Tectonics of the western margin of the Shan plateau (central Myanmar): implication for the India–Indochina oblique convergence since the Oligocene. J. Asian Earth Sci. 21, 1139–1157. https://doi.org/10.1016/S1367-9120(02)00183-9.

Besset, M., Anthony, E.J., Dussouillez, P., Goichot, M., 2017. The impact of Cyclone Nargis on the Ayeyarwady (Irrawaddy) River delta shoreline and nearshore zone (Myanmar): towards degraded delta resilience? Compt. Rend. Geosci. Vulnerability of Inter-Tropical Littoral Areas 349, 238–247. https://doi.org/10.1016/j.crte.2017.09.002.

Bianchi, T.S., 2011. The role of terrestrially derived organic carbon in the coastal ocean: a changing paradigm and the priming effect. PNAS 108, 19473–19481. https://doi.org/10.1073/pnas.1017982108.

Bianchi, T.S., 2016. Deltas and Humans: A Long Relationship Now Threatened by Global Change. Oxford University Press, New York, NY.

Bianchi, T.S., Allison, M.A., 2009. Large-river delta-front estuaries as natural "recorders" of global environmental change. PNAS 106, 8085–8092. https://doi.org/10.1073/pnas.0812878106.

Bianchi, T.S., Cui, X., Blair, N.E., Burdige, D.J., Eglinton, T.I., Galy, V., 2018. Centers of organic carbon burial and oxidation at the land-ocean interface. Org. Geochem. 115, 138–155. https://doi.org/10.1016/j.orggeochem.2017.09.008.

Binh, D.V., Kantoush, S., Sumi, T., 2020. Changes to long-term discharge and sediment loads in the Vietnamese Mekong Delta caused by upstream dams. Geomorphology 353, 107011. https://doi.org/10.1016/j.geomorph.2019.107011.

Bird, M.I., Robinson, R.A.J., Win Oo, N., Maung Aye, M., Lu, X.X., Higgitt, D.L., Swe, A., Tun, T., Lhaing Win, S., Sandar Aye, K., Mi Mi Win, K., Hoey, T.B., 2008. A preliminary estimate of organic carbon transport by the Ayeyarwady (Irrawaddy) and Thanlwin (Salween) Rivers of Myanmar. Quat. Int. Larger Asian Rivers and Their Interactions with Estuaries and Coasts 186, 113–122. https://doi.org/10.1016/j.quaint.2007.08.003.

Blair, N.E., Aller, R.C., 2012. The fate of terrestrial organic carbon in the marine environment. Annu. Rev. Mar. Sci. 4, 401–423. https://doi.org/10.1146/annurev-marine-120709-142717.

Burdige, D.J., 2005. Burial of terrestrial organic matter in marine sediments: a re-assessment: terrestrial organic matter in marine sediments. Glob. Biogeochem. Cycles 19. https://doi.org/10.1029/2004GB002368.

Chapman, H., Bickle, M., Thaw, S.H., Thiam, H.N., 2015. Chemical fluxes from time series sampling of the Irrawaddy and Salween Rivers, Myanmar. Chem. Geol. 401, 15–27. https://doi.org/10.1016/j.chemgeo.2015.02.012.

Chen, D., Li, X., Saito, Y., Liu, J.P., Duan, Y., Liu, S., Zhang, L., 2020. Recent evolution of the Irrawaddy (Ayeyarwady) Delta and the impacts of anthropogenic activities: a review and remote sensing survey. Geomorphology 365, 107231. https://doi.org/10.1016/j.geomorph.2020.107231.

Curray, J.R., 2005. Tectonics and history of the Andaman Sea region. J. Asian Earth Sci. 25, 187–232. https://doi.org/10.1016/j.jseaes.2004.09.001.

Damodararao, K., Singh, S.K., Rai, V.K., Ramaswamy, V., Rao, P.S., 2016. Lithology, monsoon and sea-surface current control on provenance, dispersal and deposition of sediments over the Andaman Continental Shelf. Front. Mar. Sci. 3 https://doi.org/10.3389/fmars.2016.00118.

Day, J.W., Gunn, J.D., Folan, W.J., Yáñez-Arancibia, A., Horton, B.P., 2007. Emergence of complex societies after sea level stabilized. Eos Trans. AGU 88, 169–170. https://doi.org/10.1029/2007EO150001.

Dean, W.E., Gorham, E., 1998. Magnitude and significance of carbon burial in lakes, reservoirs, and peatlands, p. 4.

Deng, B., Zhang, J., Wu, Y., 2006. Recent sediment accumulation and carbon burial in the East China Sea: sediment and carbon burial in the ECS. Glob. Biogeochem. Cycles 20. https://doi.org/10.1029/2005GB002559.

Dietrich, W.E., Dunne, T., Humphrey, N.F., Reid, L.M., 1982. Construction of sediment budgets for drainage basins. In: Sediment budgets and routing in forested drainage basins. USDA Forest Service Technical Report PNW-141, Vol. 141, pp. 5–23.

Dukat, D.A., Kuehl, S.A., 1995. Non-steady-state 210Pb flux and the use of 228Ra/226Ra as a geochronometer on the Amazon continental shelf. Mar. Geol. 125, 329–350. https://doi.org/10.1016/0025-3227(95)00018-T.

Edmonds, D.A., Caldwell, R.L., Brondizio, E.S., Siani, S.M.O., 2020. Coastal flooding will disproportionately impact people on river deltas. Nat. Commun. 11, 4741. https://doi.org/10.1038/s41467-020-18531-4.

Estoque, R.C., Myint, S.W., Wang, C., Ishtiaque, A., Aung, T.T., Emerton, L., Ooba, M., Hijioka, Y., Mon, M.S., Wang, Z., Fan, C., 2018. Assessing environmental impacts

and change in Myanmar's mangrove ecosystem service value due to deforestation (2000-2014). Glob. Chang. Biol. 24, 5391–5410. https://doi.org/10.1111/gcb.14409.

Fair, M.J., 2021. Sediment Transport and Trapping on the Ayeyrawady-Martaban Continetal Shelf. Unpublished master's Thesis. Virginia Institute of Marine Science, College of William and Mary.

Fontugne, M.R., Duplessy, J.-C., 1986. Variations of the monsoon regime during the upper quaternary: evidence from carbon isotopic record of organic matter in North Indian Ocean sediment cores. Palaeogeogr. Palaeoclimatol. Palaeoecol. 56, 69–88. https://doi.org/10.1016/0031-0182(86)90108-2.

Furuichi, T., Win, Z., Wasson, R.J., 2009. Discharge and suspended sediment transport in the Ayeyarwady River, Myanmar: centennial and decadal changes. Hydrol. Process. 23, 1631–1641.

Galy, V., France-Lanord, C., Beyssac, O., Faure, P., Kudrass, H., Palhol, F., 2007. Efficient organic carbon burial in the Bengal fan sustained by the Himalayan erosional system. Nature 450, 407–410. https://doi.org/10.1038/nature06273.

Garzanti, E., Wang, J.-G., Vezzoli, G., Limonta, M., 2016. Tracing provenance and sediment fluxes in the Irrawaddy River basin (Myanmar). Chem. Geol. 440, 73–90. https://doi.org/10.1016/j.chemgeo.2016.06.010.

Gibbs, R.J., 1981. Sites of river-derived sedimentation in the ocean. Geology 9, 77–80. https://doi.org/10.1130/0091-7613(1981)9<77:SORSIT>2.0.CO;2.

Giosan, L., Naing, T., Min Tun, M., Clift, P.D., Filip, F., Constantinescu, S., Khonde, N., Blusztajn, J., Buylaert, J.-P., Stevens, T., Thwin, S., 2018. On the Holocene evolution of the Ayeyawady megadelta. Earth Surface Dynam. 6, 451–466. https://doi.org/10.5194/esurf-6-451-2018.

Glover, H.E., Ogston, A.S., Fricke, A.T., Nittrouer, C.A., Aung, C., Naing, T., Kyu Kyu, K., Htike, H., 2021. Connecting sediment retention to distributary-channel hydrodynamics and sediment dynamics in a tide-dominated delta: the Ayeyarwady Delta, Myanmar. J. Geophys. Res. Earth Surf. 126 https://doi.org/10.1029/2020JF005882.

Goodbred, S.L., Kuehl, S.A., 1999. Holocene and modern sediment budgets for the Ganges-Brahmaputra river system: evidence for highstand dispersal to flood-plain, shelf, and deep-sea depocenters. Geology 27, 559–562. https://doi.org/10.1130/0091-7613(1999)027<0559:HAMSBF>2.3.CO;2.

Griffith, D.R., Martin, W.R., Eglinton, T.I., 2010. The radiocarbon age of organic carbon in marine surface sediments. Geochim. Cosmochim. Acta 74, 6788–6800. https://doi.org/10.1016/j.gca.2010.09.001.

Grill, G., Lehner, B., Thieme, M., Geenen, B., Tickner, D., Antonelli, F., Babu, S., Borrelli, P., Cheng, L., Crochetiere, H., Ehalt Macedo, H., Filgueiras, R., Goichot, M., Higgins, J., Hogan, Z., Lip, B., McClain, M.E., Meng, J., Mulligan, M., Nilsson, C., Olden, J.D., Opperman, J.J., Petry, P., Reidy Liermann, C., Sáenz, L., Salinas-Rodríguez, S., Schelle, P., Schmitt, R.J.P., Snider, J., Tan, F., Tockner, K., Valdujo, P. H., van Soesbergen, A., Zarfl, C., 2019. Mapping the world's free-flowing rivers. Nature 569, 215–221. https://doi.org/10.1038/s41586-019-1111-9.

Gupta, H., Kao, S.-J., Dai, M., 2012. The role of mega dams in reducing sediment fluxes: a case study of large Asian rivers. J. Hydrol. 464–465, 447–458. https://doi.org/10.1016/j.jhydrol.2012.07.038.

Harris, C.K., Wacht, J.T., Fair, M.J., Cote, J.M., 2022. ADCP observations of currents and suspended sediment in the macrotidal Gulf of Martaban, Myanmar. Front. Ear. Sci. 507. https://doi.org/10.3389/feart.2022.820326.

Hedges, J.I., 1992. Global biogeochemical cycles: progress and problems. Mar. Chem. 39, 67–93. https://doi.org/10.1016/0304-4203(92)90096-S.

Hedley, P.J., Bird, M.I., Robinson, R.A.J., 2009. Evolution of the Irrawaddy delta region since 1850: Evolution of the Irrawaddy delta region since 1850. Geogr. J. 176, 138–149. https://doi.org/10.1111/j.1475-4959.2009.00346.x.

Hennig, T., 2016. Damming the transnational Ayeyarwady basin. Hydropower and the water-energy nexus. Renew. Sust. Energ. Rev. 65, 1232–1246. https://doi.org/10.1016/j.rser.2016.07.048.

IOC, IHO, BODC, 2003. "Centenary Edition of the GEBCO Digital Atlas", Published on CD-ROM on Behalf of the Intergovernmental Oceanographic Commission and the International Hydrographic Organization as Part of the General Bathymetric Chart of the Oceans. British Oceanographic Data Centre, Liverpool.

Jia, J., Gao, J., Cai, T., Li, Y., Yang, Y., Wang, Y.P., Xia, X., Li, J., Wang, A., Gao, S., 2018. Sediment accumulation and retention of the Changjiang (Yangtze River) subaqueous delta and its distal muds over the last century. Mar. Geol. 401, 2–16. https://doi.org/10.1016/j.margeo.2018.04.005.

Kineke, G.C., Sternberg, R.W., 1995. Distribution of fluid muds on the Amazon continental shelf. Mar. Geol. 125, 193–233. https://doi.org/10.1016/0025-3227(95)00013-O. Geological Significance of Sediment Transport and Accumulation on the Amazon Continental Shelf.

Komada, T., Anderson, M.R., Dorfmeier, C.L., 2008. Carbonate removal from coastal sediments for the determination of organic carbon and its isotopic signatures, $\delta^{13}$C and $\Delta^{14}$C: comparison of fumigation and direct acidification by hydrochloric acid: carbonate removal from coastal sediments. Limnol. Oceanogr. Methods 6, 254–262. https://doi.org/10.4319/lom.2008.6.254.

Kuehl, S.A., DeMaster, D.J., Nittrouer, C.A., 1986. Nature of sediment accumulation on the Amazon continental shelf. Continental Shelf Res. 6, 209–225. https://doi.org/10.1016/0278-4343(86)90061-0. Sedimentary Processes on the Amazon Continental Shelf.

Kuehl, S.A., Pacioni, T.D., Rine, J.M., 1995. Seabed dynamics of the inner Amazon continental shelf: temporal and spatial variability of surficial strata. Mar. Geol. 125, 283–302. https://doi.org/10.1016/0025-3227(95)00016-R.

Kuehl, S.A., Williams, J., Liu, J.P., Harris, C., Aung, D.W., Tarpley, D., Goodwyn, M., Aye, Y.Y., 2019. Sediment dispersal and accumulation off the Ayeyarwady delta – Tectonic and oceanographic controls. Mar. Geol. 417, 106000 https://doi.org/10.1016/j.margeo.2019.106000.

Leithold, E.L., Blair, N.E., Wegmann, K.W., 2016. Source-to-sink sedimentary systems and global carbon burial: a river runs through it. Earth Sci. Rev. 153, 30–42. https://doi.org/10.1016/j.earscirev.2015.10.011.

Liu, S.M., Hong, G.-H., Zhang, J., Ye, X.W., Jiang, X.L., 2009. Nutrient budgets for large Chinese estuaries. Biogeosciences 6, 2245–2263. https://doi.org/10.5194/bg-6-2245-2009.

Liu, F., Yang, Q., Chen, S., Luo, Z., Yuan, F., Wang, R., 2014. Temporal and spatial variability of sediment flux into the sea from the three largest rivers in China. J. Asian Earth Sci. 87, 102–115. https://doi.org/10.1016/j.jseaes.2014.02.017.

Liu, J.P., Kuehl, S.A., Pierce, A.C., Williams, J., Blair, N.E., Harris, C., Aung, D.W., Aye, Y. Y., 2020. Fate of Ayeyarwady and Thanlwin rivers sediments in the Andaman Sea and Bay of Bengal. Mar. Geol. 423, 106137 https://doi.org/10.1016/j.margeo.2020.106137.

McKee, B.A., Aller, R.C., Allison, M.A., Bianchi, T.S., Kineke, G.C., 2004. Transport and transformation of dissolved and particulate materials on continental margins influenced by major rivers: benthic boundary layer and seabed processes. Cont. Shelf Res. 24, 899–926. https://doi.org/10.1016/j.csr.2004.02.009.

Meade, R.H., 1996. River-sediment inputs to major deltas. In: Milliman, J.D., Haq, B.U. (Eds.), Sea-Level Rise and Coastal Subsidence: Causes, Consequences, and Strategies, Coastal Systems and Continental Margins. Springer, Netherlands, Dordrecht, pp. 63–85. https://doi.org/10.1007/978-94-015-8719-8_4.

Milliman, J.D., Farnsworth, K.L., 2011. River Discharge to the Coastal Ocean: A Global Synthesis. Cambridge University Press, Cambridge. https://doi.org/10.1017/CBO9780511781247.

Milliman, J.D., Meade, R.H., 1983. World-wide delivery of river sediment to the oceans. J. Geol. 91, 1–21.

Mitchell, A.H.G., 1993. Cretaceous–Cenozoic tectonic events in the western Myanmar (Burma)–Assam region. J. Geol. Soc. 150, 1089–1102. https://doi.org/10.1144/gsjgs.150.6.1089.

Nienhuis, J.H., Ashton, A.D., Edmonds, D.A., Hoitink, A.J.F., Kettner, A.J., Rowland, J. C., Törnqvist, T.E., 2020. Global-scale human impact on delta morphology has led to net land area gain. Nature 577, 514–518. https://doi.org/10.1038/s41586-019-1905-9.

Nittrouer, C.A., Kuehl, S.A., DeMaster, D.J., Kowsmann, R.O., 1986. The deltaic nature of Amazon shelf sedimentation. GSA Bull. 97, 444–458. https://doi.org/10.1130/0016-7606(1986)97<444:TDNOAS>2.0.CO;2.

Nittrouer, C.A., Kuehl, S.A., Sternberg, R.W., Figueiredo, A.G., Faria, L.E.C., 1995. An introduction to the geological significance of sediment transport and accumulation on the Amazon continental shelf. Mar. Geol. 125, 177–192. https://doi.org/10.1016/0025-3227(95)00075-A.

Nittrouer, C.A., Kuehl, S.A., Figueiredo, A.G., Allison, M.A., Sommerfield, C.K., Rine, J. M., Faria, L.E.C., Silveira, O.M., 1996. The geological record preserved by Amazon shelf sedimentation. Cont. Shelf Res. 16, 817–841. https://doi.org/10.1016/0278-4343(95)00053-4.

Nittrouer, C.A., DeMaster, D.J., Kuehl, S.A., Figueiredo, A.G., Sternberg, R.W., Faria, L.E. C., Silveira, O.M., Allison, M.A., Kineke, G.C., Ogston, A.S., Souza Filho, P.W.M., Asp, N.E., Nowacki, D.J., Fricke, A.T., 2021. Amazon sediment transport and accumulation along the continuum of mixed fluvial and marine processes. Annu. Rev. Mar. Sci. 13, 501–536. https://doi.org/10.1146/annurev-marine-010816-060457.

Park, E., Lim, J., Ho, H.L., Herrin, J., Chitwatkulsiri, D., 2021. Source-to-sink sediment fluxes and budget in the Chao Phraya River, Thailand: a multi-scale analysis based on the national dataset. J. Hydrol. 594, 125643 https://doi.org/10.1016/j.jhydrol.2020.125643.

Potemra, J.T., Luther, M.E., O'Brien, J.J., 1991. The seasonal circulation of the upper ocean in the Bay of Bengal. J. Geophys. Res. Oceans 96, 12667–12683. https://doi.org/10.1029/91JC01045.

Ramaswamy, V., Rao, P.S., 2014. The Myanmar Continental Shelf. The Geological Society of London.

Ramaswamy, V., Rao, P.S., Rao, K.H., Thwin, S., Rao, N.S., Raiker, V., 2004. Tidal influence on suspended sediment distribution and dispersal in the northern Andaman Sea and Gulf of Martaban. Mar. Geol. 208, 33–42. https://doi.org/10.1016/j.margeo.2004.04.019.

Qiao, S., Shi, X., Wang, G., Zhou, L., Hu, B., Hu, L., Yang, G., Liu, Y., Yao, Z., Liu, S., 2017. Sediment accumulation and budget in the Bohai Sea, Yellow Sea and East China Sea. Marine Geology 390, 270–281. https://doi.org/10.1016/j.margeo.2017.06.004.

Ramaswamy, V., Gaye, B., Shirodkar, P., Rao, P., Chivas, A., Wheeler, D., Thwin, S., 2008. Distribution and sources of organic carbon, nitrogen and their isotopic signatures in sediments from the Ayeyarwady (Irrawaddy) continental shelf, northern Andaman Sea. Faculty of Science - Papers (Archive) 137–150. https://doi.org/10.1016/j.marchem.2008.04.006.

Ramos-Scharrón, C.E., MacDonald, L.H., 2007. Development and application of a GIS-based sediment budget model. J. Environ. Manag. 84, 157–172. https://doi.org/10.1016/j.jenvman.2006.05.019.

Rao, P.S., Ramaswamy, V., Thwin, S., 2005. Sediment texture, distribution and transport on the Ayeyarwady continental shelf, Andaman Sea. Mar. Geol. 216, 239–247. https://doi.org/10.1016/j.margeo.2005.02.016.

Richards, D.R., Friess, D.A., 2015. Rates and drivers of mangrove deforestation in Southeast Asia, 2000–2012. PNAS 113 (2), 344–349. https://doi.org/10.1073/pnas.1510272113.

Robinson, R.A.J., Bird, M.I., Oo, N.W., Hoey, T.B., Aye, M.M., Higgitt, D.L., X. X., L, Swe, A., Tun, T., Win, S.L., 2007. The Irrawaddy River sediment flux to the Indian Ocean: the original nineteenth-century data revisited. J. Geol. 115, 629–640. https://doi.org/10.1086/521607.

Rodolfo, K.S., 1969a. Sediments of the Andaman Basin, northeastern Indian Ocean. Mar. Geol. 7, 371–402. https://doi.org/10.1016/0025-3227(69)90014-0.

Rodolfo, K.S., 1969b. Bathymetry and marine geology of the Andaman Basin, and tectonic implications for southeast Asia. GSA Bull. 80, 1203–1230. https://doi.org/10.1130/0016-7606(1969)80[1203:BAMGOT]2.0.CO;2.

Rosati, J.D., 2005. Concepts in sediment budgets. J. Coast. Res. 307–322. https://doi.org/10.2112/02-475A.1.

Saito, Y., 2007. Shrinking Megadeltas in Asia: Sea-Level Rise and Sediment Reduction Impacts from Case Study of the Chao Phraya Delta.

Saito, Y., 2021. Asian delta evolution in response to sea-level changes. In: Source-to-Sink Delta Seminar Series. Youtube.com.

Saito, Y., Yang, Z., 1995. Historical change of the Huanghe (Yellow River) and its impact on the sediment budget of the East China Sea. In: Tsunogai, S., Iseki, K., Koike, I., Oba, T. (Eds.), Global Fluxes of Carbon and Its Realted Substances in the Coastal Sea-Ocean-Atmosphere System. M and J International, Yokohama, pp. 7–12.

Shimozono, T., Tajima, Y., Akamatsu, S., Matsuba, Y., Kawasaki, A., 2019. Large-scale channel migration in the Sittang River Estuary. Sci. Rep. 9, 9862. https://doi.org/10.1038/s41598-019-46300-x.

Showers, W.J., Angle, D.G., 1986. Stable isotopic characterization of organic carbon accumulation on the Amazon continental shelf. Cont. Shelf Res. 6, 227–244. https://doi.org/10.1016/0278-4343(86)90062-2.

Sloan, R.A., Elliott, J.R., Searle, M.P., Morley, C.K., 2017. Chapter 2 active tectonics of Myanmar and the Andaman Sea. Geol. Soc. Lond. Mem. 48, 19–52. https://doi.org/10.1144/M48.2.

Soe, H.K., Hammond, C., 2019. Myanmar's Ayeyarwady River at Risk from Rampant Sand Mining (Earth Journalism Network, 2019).

Stamp, L.D., 1940. The Irrawaddy River. Geogr. J. 95, 329. https://doi.org/10.2307/1787471.

Stanley, D.J., Warne, A.G., 1994. Worldwide initiation of holocene marine deltas by deceleration of sea-level rise. Science 265, 228–231. https://doi.org/10.1126/science.265.5169.228.

Stanley, D.J., Warne, A.G., 1997. Holocene sea-level change and early human utilization of deltas. GSA Today 7 (12), 1–7.

Stephenson, D., Marshall, T.R., 1984. The petrology and mineralogy of Mt. Popa Volcano and the nature of the late-Cenozoic Burma Volcanic Arc. J. Geol. Soc. 141, 747–762. https://doi.org/10.1144/gsjgs.141.4.0747.

Syvitski, J.P.M., 2008. Deltas at risk. Sustain. Sci. 3, 23–32. https://doi.org/10.1007/s11625-008-0043-3.

Syvitski, J.P.M., Saito, Y., 2007. Morphodynamics of deltas under the influence of humans. Glob. Planet. Chang. 57, 261–282. https://doi.org/10.1016/j.gloplacha.2006.12.001.

Syvitski, J.P.M., Kettner, A.J., Overeem, I., Hutton, E.W.H., Hannon, M.T., Brakenridge, G.R., Day, J., Vörösmarty, C., Saito, Y., Giosan, L., Nicholls, R.J., 2009. Sinking deltas due to human activities. Nat. Geosci. 2, 681–686. https://doi.org/10.1038/ngeo629.

Ve, N.D., Fan, D., Van Vuong, B., Lan, T.D., 2021. Sediment budget and morphological change in the Red River Delta under increasing human interferences. Mar. Geol. 431, 106379 https://doi.org/10.1016/j.margeo.2020.106379.

Vigny, C., Socquet, A., Rangin, C., Chamot-Rooke, N., Pubellier, M., Bouin, M.-N., Bertrand, G., Becker, M., 2003. Present-day crustal deformation around Sagaing fault, Myanmar. J. Geophys. Res. Solid Earth 108. https://doi.org/10.1029/2002JB001999.

Warrick, J.A., 2014. Eel River margin source-to-sink sediment budgets: revisited. Mar. Geol. 351, 25–37. https://doi.org/10.1016/j.margeo.2014.03.008.

Webb, E.L., Jachowski, N.R.A., Phelps, J., Friess, D.A., Than, M.M., Ziegler, A.D., 2014. Deforestation in the Ayeyarwady Delta and the conservation implications of an internationally-engaged Myanmar. Glob. Environ. Chang. 24, 321–333. https://doi.org/10.1016/j.gloenvcha.2013.10.007.

Xue, Z., Liu, J.P., DeMaster, D., Van Nguyen, L., Ta, T.K.O., 2010. Late Holocene evolution of the Mekong subaqueous delta, southern Vietnam. Mar. Geol. 269, 46–60. https://doi.org/10.1016/j.margeo.2009.12.005.

Yang, S.L., Milliman, J.D., Li, P., Xu, K., 2011. 50,000 dams later: erosion of the Yangtze River and its delta. Glob. Planet. Chang. 75, 14–20. https://doi.org/10.1016/j.gloplacha.2010.09.006.

Zhou, L., Liu, J., Saito, Y., Diao, S., Gao, M., Qiu, J., Xu, C., He, L., Ye, S., 2020. Sediment budget of the Yellow River delta during 1959–2012, estimated from morphological changes and accumulation rates. Mar. Geol. 430, 106363 https://doi.org/10.1016/j.margeo.2020.106363.

World Population Review, 2019. Myanmar population 2020. http://worldpopulationreview.com/countries/myanmar-population/ (accessed 14 Jan 2020).